LBNL-40721
UC-1501

ERNEST ORLANDO LAWRENCE
BERKELEY NATIONAL LABORATORY

Advanced Anode Materials for Li-Ion Batteries

K. Kinoshita

Environmental Energy Technologies Division

October 1997

To be published as a chapter in *New Trends in Electrochemical Technology: Energy Storage Systems for Electronics*, T. Osaka and M. Datta, Eds., Gordon & Breach Science, Reading, UK, 1998

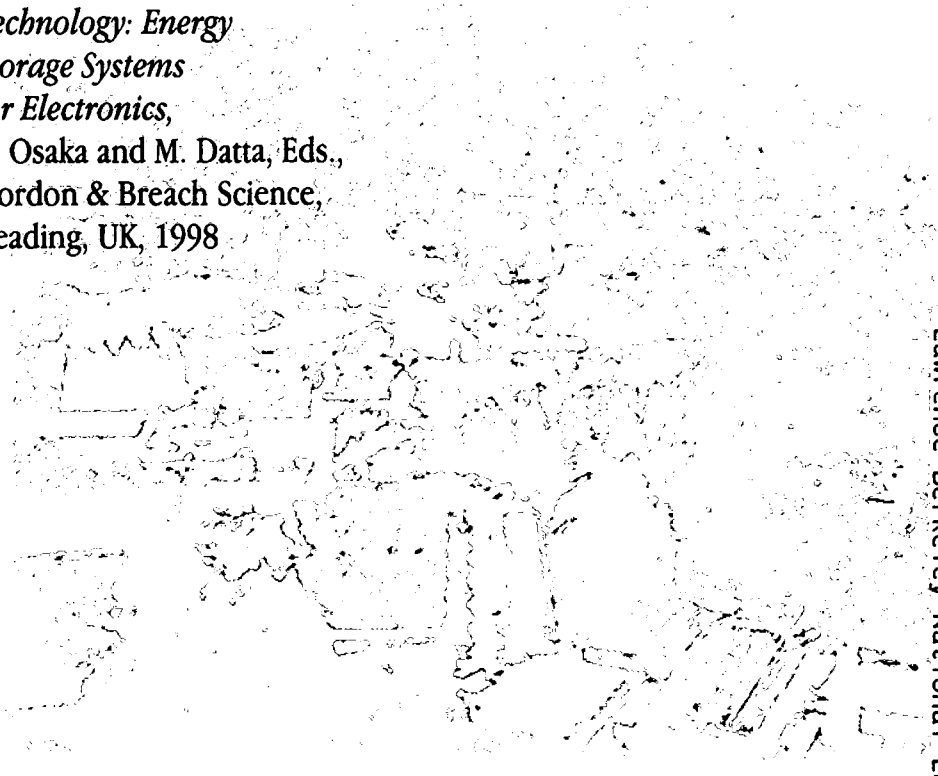

DISCLAIMER

LBNL-40721
UC-1501

Advanced Anode Materials for Li-Ion Batteries

by

K. Kinoshita

Environmental Energy Technologies Division
Lawrence Berkeley National Laboratory
Berkeley, California 94720

October 1997

This work was supported by the Assistant Secretary for Energy Efficiency and Renewable Energy, Office of Transportation Technologies, Office of Advanced Automotive Technologies of the U.S. Department of Energy under Contract No. DE-AC03-76SF00098.
This paper was submitted as a chapter in "New Trends in Electrochemical Technology," Gordon and Breach Science Publishers, Reading, United Kingdom.

1. INTRODUCTION

The commercialization of lithium-ion cells in the early 1990's by Sony Corporation has led to a major expansion in the application of rechargeable Li batteries for portable electronic devices. Until the advent of the rechargeable Li-ion cell, the only Li cells that were commercially available were primary cells. The successful utilization of a carbon host to store Li ions in the rechargeable negative electrode has led to the commercial development of Li-ion cells. However, the original research on storing Li ions by intercalation in graphite was reported much earlier, and these studies paved the way for the successful implementation of carbon in Li-ion cells.

Prior to the success of Li-ion technology, attempts to produce rechargeable Li cells were frustrated by technical issues related to safety and the poor cycle life of the Li electrode. The morphological changes that occur by repetitive charge/discharge cycling of Li eventually led to cell failure. To overcome some of these problems, alloys of Li, such as Li-Al and Li-Si, were considered. Here again problems were encountered with mechanical stability of the alloys when the electrode was cycled. The technology relevant to rechargeable Li cells is described extensively elsewhere (for example, in other chapters in this book) and will not be discussed here. To date, Li metal and Li alloys in nonaqueous liquid electrolytes have shown limited promise in practical rechargeable cells.

Storage of Li in carbon to form the negative electrode in Li-ion cells occurs by different mechanisms, which are discussed in this review. The terminology which is used to describe the mechanism by which Li storage takes place in carbonaceous materials is not consistent, and may lead to confusion. The term "intercalation" is often widely used to describe the Li storage mechanism. An International Committee for Characterization and Terminology of Carbon and Graphite has presented nomenclature and terminology which refer to graphite intercalation compounds. In the report by Boehm *et al.* (1) the verb to intercalate is defined as "the process of inserting a substance between the carbon sheets of the graphite lattice." Correspondingly, it is accepted that the process of removing the substance is to "de-intercalate." However, as will be discussed later, Li storage in carbon may involve processes that do not involve intercalation. In this case, the term "insertion" and "de-insertion", respectively, will be used.

In this review, the emphasis of the discussion is on the properties and use of carbonaceous materials in the negative electrodes of Li-ion cells. A brief discussion of alternative electrode materials to carbon for Li-ion cells will also be presented.

1.1. Carbon in Li-Ion Cells

The theoretical capacity of Li metal is considerably higher than that of lithiated graphite (LiC_6), 3862 mAh/g *vs.* 372 mAh/g. However, the practical specific capacities are very comparable if a large excess of Li metal (*i.e.,* 5-fold excess) is used in rechargeable Li cells, as illustrated in Table 1. Furthermore, the practical capacity density of graphite can exceed that of metallic Li in a 5-fold excess. If capacities greater than 372 mAh/g are attained with amorphous carbon electrodes, they would provide a more competitive specific energy to that of Li metal. It is apparent from the comparison in Table 1 that lithiated carbons provide an extremely attractive alternative to Li metal for rechargeable Li batteries. However, the operating potential of both graphitic and amorphous carbons should be limited to > 0 V (*vs.* Li/Li^+) to avoid deposition of metallic Li.

The overall charge (Li intercalation in carbon, de-intercalation of metal oxide) reaction in a Li-ion cell that contains graphitic carbon and a lithiated metal oxide (MO_2, M = Co, Ni, or Mn) is

$$LiMO_2 + 6C \rightarrow Li_{1-x}MO_2 + Li_xC_6 \qquad [A]$$

During charge, Li from the metal oxide is transferred to the carbon to form the negative electrode. Correspondingly, discharge (de-intercalation of Li from carbon) of Li-ion cells involves the reverse reaction. This transport of Li back and forth during the charge and discharge processes has led to the use of terminology such as "rocking chair", "shuttlecock", "SWING", etc. to describe Li-ion cells. According to Scrosati (2), the term "rocking chair battery" was first suggested by Armand (3). Ohzuku and co-workers (4) have used the term shuttlecock cell and Brandt *et al.* (5) refer to similar cells as SWING systems.

In commercial cells, $LiCoO_2$ is the dominant lithiated metal oxide in the positive electrode. The Li-ion cell is fabricated in the discharged state where the two electrode components are stable in the ambient air environment. In the case of positive electrodes, a variety of lithiated metal oxides such as $Li_{1-y}CoO_2$ ($0 < y < 0.8$), $Li_{1-y}NiO_2$ ($0 < y < 0.8$) and $Li_{1-y}Mn_2O_4$ ($0 < y < 1$) are available (6). Reviews of carbon technology relevant to Li-ion cells are presented by Megahed and Scrosati (7), Besenhard (7), Tarascon and Guyomard (9), Houssain (10), etc.

1.2. Historical Perspective

Herold (11) is generally credited with reporting the first synthesis of Li-intercalated graphite in 1955. These samples were made by contacting graphite with liquid or gaseous Li. Following the discovery that Li intercalation compounds can be formed with graphite, there was interest in this material by researchers who were seeking new types of electronic conductors with low mass density. The solid-state properties of Li-intercalated graphite were extensively studied by several research groups, notably by Fischer and co-workers (12-35) and Billaud and Herold (36-38). A graphic representation of the number of technical publications on Li-intercalated carbons during the period from 1975 to 1996 is presented in Figure 1. This graph is not intended to be exhaustive, but rather to illustrate the level of activity on Li-intercalated carbons. Much of the research on the solid-state properties of Li-intercalated graphite occurred in the late 1970's and appeared in print during the early 1980's. However, much of this effort diminished by the mid and late 1980's. There was a dramatic increase in the number of publications on Li-intercalated carbon for Li-ion cells in the latter half of the 1980's, and this is illustrated by the change in the plot in Figure 1. The data in Figure 1 shows a decrease in the number of publications in 1996, but this may be an artifact of the method used to search the published literature.

The background events that led to the use of Li-intercalated carbons in electrodes for Li-ion cells are a subject of debate. In what follows is the author's interpretation of the events leading up to the commercialization of Li-ion cells. In 1970, Dey and Sullivan (39) published their observations on the electrochemical decomposition of propylene carbonate (PC) on graphite electrodes. They reported that PC decomposes to propylene gas and Li_2CO_3 during cathodic charging at approximately 0.6 V (*vs.* Li/Li^+) and that the graphite electrode disintegrates slowly. Both of these phenomena have been observed subsequently with graphite for Li-ion cells using PC as the solvent. Shortly after the report by Dey and Sullivan, Dunning et al. (40) published their experimental results on a Li (-)/$LiClO_4$-dimethyl sulfite (DMS)/graphite (+) cell. When graphite was used as the electrode, the authors concluded that Li intercalation did not take place. However, in other tests, swelling of the graphite electrode was observed during cell charging. The formation of a perchlorate-intercalated graphite was proposed. Near the mid 1970's, Besenhard (41,42) reported observations of electrochemical intercalation of alkali metal in graphite that is immersed in a nonaqueous electrolyte. Cyclic voltammetry of graphite in dimethylsulfoxide (DMSO), 1,2-dimethoxyethane (DME) or PC indicated reversible electrochemical reduction occurs at potentials more positive than that for Li deposition, which was attributed to an intercalation reaction involving Li. Steps were observed in the potential-time curves during galvanostatic reaction of graphite in $LiClO_4$-DME or $LiClO_4$-DMSO, indicative of the staging phenomenon during Li intercalation. About the same time, Eichinger (43) also

reported that graphite electrodes are capable of reversible reactions involving the intercalation and de-intercalation of Li ions.

It was during the late 1970's that Armand and Touzain (44) reviewed the application of intercalation compounds for battery electrode materials. They suggested that some graphite intercalation compounds may be good candidates as cathode materials (positive electrode) in high-energy-density batteries. Experimental cell were constructed, and electrochemical results were obtained in Li/1 M $LiClO_4$/LiX cells (LiX = $C_{25}AuCl_3$, $C_{10}CuCl_2$, $C_{21}TiF_4$, $C_{11}FeCl_3$, $C_{29}CrCl_3$). In addition, they suggested that ionic intercalation compounds, such as alkali metal compounds that include K and Li, could be used as an anode material (negative electrode). In 1979, Pfluger et al. (45) demonstrated that highly oriented pyrolytic graphite (HOPG, Union Carbide) can be electrochemically intercalated with Li in a nonaqueous electrolyte containing a Li salt to form different compounds such as LiC_6 and LiC_{12}. They observed that intercalation of Li in HOPG produced a color change from black to golden yellow by applying a voltage of 3-5 V. On reversing the polarity, the HOPG changed color from golden yellow to black. These experiments demonstrated the electrochromic effect based on Li intercalation of graphite.

In the early 1980's, two U.S. Patents were issued to Basu (46,47) which described the use of Li-intercalated graphite (LiC_6) for electrodes in molten salt (LiCl or LiCl-KCl) and nonaqueous (1,3-dioxolane) batteries. These patents were followed by other U.S. patents in the mid 1980's, and a large number of U.S. patents were issued in the 1990's. Of the many U.S. patents on carbon materials for Li-ion cells, the largest number is issued to Japanese companies. Following this trend has been the proliferation in the number of technical publications since about 1985 by Japanese researchers (included in Figure 1), about three times greater than the number of publications from U.S. researchers. This may help explain the dominance of Japanese companies in the commercialization of Li-ion cells for the consumer market.

2. STRUCTURE OF CARBON AND LITHIATED CARBON

A detailed discussion on the physicochemical properties of carbons for electrochemical applications is presented by Kinoshita (48). Therefore, only a brief summary of the physicochemical properties of carbon is presented here.

2.1. Crystallographic Structure

Elemental carbon is found in three major crystallographic structures: (i) diamond, (ii) buckminsterfullerene and (iii) graphite. Diamond has a tetrahedral structure with covalent bonds (sp^3-hybridization). Buckminsterfullerene ("fullerene") in its common form, C_{60}, resembles a soccer ball consisting of carbon atoms in pentagonal and hexagonal arrays. Graphite in its most common structure consists of carbon atoms which are arranged in an ABAB... hexagonal structure (see Figure 2). In this crystallographic structure, the graphite layer planes [(002) spacing] are separated by 3.354 Å. Of the four valence electrons, three electrons with sp^2 hybridization from the in-plane covalent σ bonds and the other $2p_z$ electron give a π-valence band and a π^*-conduction band. The weak van der Waals bonds between the layer planes permit facile insertion of foreign ions to form intercalated graphite compounds. Graphite with a rhombohedral structure with ABCABC... arrangement is also found, but to a much lesser extent. Other variations of the graphite structure where the layer planes are separated by a distance that can exceed 3.6 Å are considered amorphous (or disordered) carbon. In amorphous carbon, the hexagonal array are not in alignment as in graphite, but instead they are rotated with respect to each other so no three dimensional order exists (see Figure 2b). This structure is often referred to as turbostratic. As might be expected, the physical properties of carbonaceous materials vary dramatically. For example, carbon blacks are available with surface areas that range from less than 10 m^2/g to over 1000 m^2/g. Correspondingly, the average particle size is >2500 Å to

<100 Å. Carbonaceous materials with much larger particle dimensions are available, such as carbon fibers which have typical diameters of 10 μm. Graphite powders are also available with average particle size of 10-100 μm. Carbon is truly an unique material with physicochemical properties that vary from the extremes of graphite to highly amorphous carbon, which have varying degrees of long- and short-range order, different bonding between the carbon atoms, different crystalline structures, and also of importance in electrochemistry, a wide range of chemical properties.

2.2. Surface Structure

As indicated in Figure 2, there are two distinct types of sites on graphite. These are the basal plane, which is the surface of the layer planes, and the edge sites, which are the termination sites of the basal plane. The anisotropic properties of carbons, particularly graphite and graphitized carbons, and their influence on electrochemical reactions are well-known. This is attributed to the existence of a crystallographic structure consisting of basal planes, which are relatively inactive, and edge plane sites, which are active for electrochemical reactions. Consequently, the electrochemical properties of carbonaceous materials are partially dictated by the relative fraction of both types of crystallographic sites. The edge sites are capable of reacting to form surface groups. Examples of typical oxygenated surface groups that have been identified at the edge sites of carbon are illustrated schematically in Figure 3. These surface groups have a major impact on the physicochemical properties of carbon. For example, the wettability of carbon in water improves when oxygen surface groups are present (49). On the other hand, carbon powders that have high oxygen content exhibit higher electrical resistivity (50). As will be discussed later, oxygen surface groups also play a role in the electrochemical behavior of carbon for Li-ion cells.

Carbonaceous materials have many desirable characteristics and physicochemical properties which have aided in the widespread acceptance of carbons in electrochemistry. For many electrochemical applications carbon is selected because of its good electrical and thermal conductivities, low density, adequate corrosion resistance, low thermal expansion, low elasticity, and high purity. In addition carbon materials can be produced in a variety of structures, *i.e.*, powders, fibers, large blocks, and thin solid and porous sheets. Furthermore, carbon materials are readily available and generally low-cost. Unfortunately, it is the wide variety of carbons which makes selection of the appropriate carbon for electrochemical systems and prediction of its electrochemical behavior sometime more difficult.

2.3. Lithiated Carbon Structure

When graphite is used as the host material, the resulting stable Li-intercalation compound has a limiting composition of LiC_6, which appears to be gold or yellow in color. At this composition, which is also called the stage-one compound, the insertion of Li results in a change in the crystallographic structure from ABABA... to AAA... Accompanying intercalation is a slight increase in the distance between the layer planes to 3.706 Å, about a 10% expansion. In this definition of a stage-one compound, the Li atoms are located between every graphite layer plane. A schematic representation of the location of Li in the layer planes of the graphite structure is illustrated in Figure 4a for LiC_6, with Li located in the center of the carbon hexagons. The unit cell for LiC_6 belongs to the P6/mmm space group with parameters $a = 4.305 \pm 0.001$ Å and $c = 3.706 \pm 0.001$ Å (51). Analysis of the molar volume of lithiated graphite indicates the volume contracts upon intercalation (52). The molar volume of the reactants Li + 6 C is 44.84 cm^3, while the corresponding volume for LiC_6 is 35.43 cm^3, a volume reduction of 21%. The formation of partial covalent bonds between Li 2s and C p_z electrons may promote volume contraction. Calculations by Holzwarth et al. (53) show clear evidence for partial covalent bonding between C and Li in LiC_6.

The schematic representation of the layer structure for various stage compounds is illustrated in Figure 4b. In the stage-two compound, the Li atoms are separated by two graphite layer planes. Two stage-two compounds exist, LiC_{18} which has no long-range order, is blue in appearance, and LiC_{12} which is an ordered commensurate in-plane, is metallic pink and copper in color. For the stage-three compound, the Li atoms are separated by three graphite layer planes, and so on.

The usual limiting composition of Li-intercalated graphite is LiC_6, with the distribution of Li in the layer planes indicated in Figure 4a. However, under more extreme conditions using high pressures, as discussed in the following section, the composition of Li-intercalated graphite can be increased beyond LiC_6 to LiC_4 and LiC_2. The arrangement of Li in these two higher compositions is illustrated in Figure 4c. Calculations by Nalimova and Semenenko (54) indicate that the density (volume Li/volume LiC_2) of Li in LiC_2 is 0.59 g/cm^3, higher than that of metallic Li, *i.e.*, 0.53 g/cm^3. NMR studies with Li^7 by Conard *et al.* (55) suggested that covalent Li-Li bonds with bond distance of 2.672 Å are present in LiC_2.

3. SYNTHESIS OF LITHIATED CARBON

Of the various types of carbon structures discussed above, only those based on the graphite structure such as the highly ordered graphites and the highly disordered carbons are practical materials for Li-ion batteries. Diamond, for obvious cost reasons, is not a practical material for Li batteries. Interest in the fullerenes for electrochemical applications has been strong. Observations by numerous research groups (56-60) suggest that the fullerenes (*i.e.*, C_{60}, C_{70}) are not likely candidates for Li batteries because of their solubility in nonaqueous electrolytes and poor electrochemical reversibility. The following discussion will focus on the intercalation of Li in carbonaceous materials, principally graphitized carbons.

3.1. Physicochemical Techniques

Table 2 summarizes some of the different non-electrochemical methods that have been reported to produce Li-intercalated carbons (electrochemical formation of Li-intercalated carbons is discussed in the following section), and the reaction can be represented as

$$xLi + 6C \rightarrow Li_xC_6 \qquad [B]$$

In most of these synthesis procedures, graphite was used as the host material for producing Li-intercalated carbon compounds. Lithium in the form of a gas, liquid or solid is capable of reacting with graphite to form an intercalated compound. Both high pressure and/or high temperature facilitate the formation of Li-intercalated graphite. However, at high temperatures (*e.g.*, >450°C), lithium carbide, Li_2C_2, is easily formed. When high pressure (40-60 kbar, 280-300°C) is used (54), the Li-intercalated compound $LiC_{2.4}$ is produced from a mixture of Li and graphite, but it is not stable at ambient pressure, decomposing rapidly to $LiC_{2.6\text{-}3.4}$, then slowly to LiC_6 when the pressure is reduced to ambient. A review on the synthesis of intercalated graphite compounds formed by high pressure was published by Clarke and Uher (79).

3.2. Electrochemical Preparation

Lithiated carbons, in which the Li species are intercalated between the layer planes (*i.e.*, in graphite) or associated with other sites (*i.e.*, in disordered carbons), are produced by both chemical and electrochemical processes. The electrochemical synthesis of Li-intercalated graphite in a nonaqueous electrolyte containing a Li salt can be represented by

$$xLi^+ + 6C + xe^- \rightarrow Li_xC_6 \qquad [C]$$

For the stage-one compound (x = 1), LiC_6, the electrochemical capacity is equivalent to 372 mAh/g C, and 186 mAh/g C for the stage-two compound (x = 0.5), LiC_{12}. The driving force for intercalation is the electrochemical potential. In the optimum case, graphite in a nonaqueous electrolyte containing a Li salt will intercalate Li ions when the potential is changed cathodically towards that of Li/Li^+. At potentials more negative than the Li/Li^+ potential, deposition of metallic Li on the graphite surface is possible.

A schematic representation of the profiles for the potential of carbon electrodes as Li ions are intercalated at constant current is illustrated in Figure 5. Typically, the potential of the carbon is >1 V before Li intercalation takes place. In the case of highly graphitized carbon, when current is applied to intercalate Li, the potential initially drops rapidly to near 0.8 V (*vs.* Li/Li^+) where electrolyte decomposition and the formation of a surface film occur. When these reactions are taking place, the potential remains close to a constant value. The duration of the potential plateau varies with extent of electrolyte decomposition. Following electrolyte decomposition, the potential declines and the majority of Li intercalation occurs at <0.25 V. With highly graphitized carbons, inflections and plateaus in the potential-composition (x) profiles are evident which are related to staging phenomena. Amorphous carbons exhibit a sloping profile, with no evidence of staging. In the extreme case, electrolyte decomposition and gas evolution can occur with little or no Li intercalation. An example of the first charge/discharge cycle observed with an amorphous carbon (obtained by chemical vapor deposition of benzene) is presented in Figure 6. The sloping potential profile for insertion/de-insertion of an amorphous carbon are clearly evident. The first charge half-cycle of carbon (Q_t) in a Li-ion cell involves Li insertion or storage in the carbon structure (Q_{in}) and electrolyte decomposition (Q_{irr}). The subsequent discharge half-cycle leads to de-insertion of Li ions (Q_{dein}) and minimal further electrolyte decomposition. The difference between the charge and discharge half-cycles ($Q_{irr} = Q_t - Q_{dein}$) is attributed to the "irreversible capacity loss", which represents the charge (coulombs) associated with electrolyte decomposition. In subsequent charge/discharge cycles, the charge capacity with a useful carbonaceous material is equal to Q_{in}, which is approximately constant with cycling and is identified with the reversible Li storage capacity ($Q_{in} = Q_{rev}$). Because the cell is manufactured in the discharged state, *i.e.*, no Li is present in the carbon structure, it is advantageous to minimize the irreversible capacity loss which reduces the amount of Li that is available for the intercalation or insertion reactions. Studies on various carbons indicate that the irreversible capacity loss increases with an increase in the surface area (80, 81).

3.3. Electrolyte Decomposition on Carbon

The electrochemical insertion of Li into carbon electrodes requires careful attention to the selection of the electrolyte composition. There are several reasons for this:

- only nonaqueous electrolytes (organic solvent based and polymer electrolyte) can be used for the electrochemical intercalation of Li into carbon because intercalated Li is very sensitive to water, hence, trace amounts of water, *e.g.*, 20 ppm, in the electrolyte cause poor performance of the electrochemical cell;
- some nonaqueous electrolytes undergo facile decomposition during electrochemical Li intercalation because the carbon surface acts as catalyst;
- some solvents may co-intercalated into graphite, resulting in the exfoliation and swelling of the structure.

For example, electrochemical intercalation is difficult with graphitized carbon in $LiClO_4$/PC because of rapid electrolyte decomposition and exfoliation of the electrode structure. Successful intercalation of Li into graphite was made possible using a mixed solvent electrolyte system such as $LiPF_6$ in EC+DEC. In contrast, $LiClO_4$ in PC is an acceptable electrolyte for the intercalation of Li in a nongraphitized carbon such as petroleum coke, but the electrochemical Li capacity is less, amounting to about 180 mAh/g C. Other amorphous carbons have been investigated, and

the electrochemical capacities are reported to exceed 372 mAh/g C, as discussed below. Naji et al. (81b) demonstrated that PC is an acceptable electrolyte solvent for Li intercalation of graphite if a "protective layer" is already present on the surface. The protective surface layer was first formed on graphite by intercalation of Li using an electrolyte of $LiClO_4$ in EC or DMC. The graphite electrode was then immersed in an electrolyte containing $LiClO_4$ in PC, where it cycled reversibly when a sufficiently thick and electrochemically protective film was present to prevent the reduction of PC.

The decomposition of nonaqueous electrolytes on graphite electrodes in Li-ion cells proceeds by electrochemical reduction reactions that form gaseous products, and products that are soluble and/or insoluble in the solvent. The solid products deposit on the carbon surface to form the solid electrolyte interphase (SEI), which may be part of a much thicker layer. This SEI plays an important role in Li-ion cells by influencing the cycle life, shelf life, safety, and charge/discharge rate and efficiency. The SEI must be a good Li^+-ion conductor but not an electronic conductor. It must also serve to restrict the transport of solvent or anions to the carbon surface. In many respects the SEI is a passive layer that prevents the surface of the carbon from acting as a site for continuing electrolyte decomposition. Takei *et al.* (82) reported that the SEI which forms on carbon black is about 10-15 Å in thickness. However, on metallic Li, the SEI is reported to be typically >20 Å, and can attain thicknesses of even >1000 Å in nonaqueous electrolytes (83).

Aurbach and co-workers (84,85) have used a variety of spectroscopic techniques to identify the numerous products that form during electrolyte decomposition. Ein-Eli *et al.* (86) have also recently summarized some of the products and reactions that occur during decomposition of various electrolytes in Li-ion cells. Based on these studies, several types of decomposition products were identified in propylene carbonate (PC), ethylene carbonate (EC) and diethyl carbonate (DEC), *e.g.*,

PC decomposition: $\rightarrow CH_3CH(OCO_2Li)CH_2OCO_2Li + CH_3CH{=}CH_2$ (gas) [D]

EC decomposition: $\rightarrow \begin{matrix} H_2C\text{-}OCO_2Li \\ | \\ H_2C\text{-}OCO_2Li \end{matrix} + CH_2{=}CH_2$ (gas) [E]

DEC decomposition: $\rightarrow CH_3CH_2OCO_2Li$ (soluble) + CH_3COLi (soluble) [F]

In addition, inorganic compounds such as Li_2CO_3, Li_2O, CO and H_2 are also produced by reactions with the organic products or trace water. Shu *et al.* (87,88) proposed the following detailed sequence of reactions for the decomposition of PC during the first charge (Li intercalation) of graphite in 1 M $LiClO_4$ - PC/EC:

Complex formation: $mPC + Li^+ \rightarrow [PC_mLi^+]$ [G]

Radical formation: $[PC_mLi^+] + e^- \rightarrow [PC_mLi^+]^{\cdot}$ [H]

Radical termination: $[PC_m\dot{L}i^+] \rightarrow$ Li alkyl carbonate [I]

Electrochemical reduction: $[PC_m\dot{L}i^+] + e^- + Li^+ \rightarrow Li_2CO_3 + C_3H_6 + (1\text{-}m)PC$ [J]

Chemical reduction: $[PC_mLi^+] + nC + e^- \rightarrow [PC_mLi^+\,C_n]^-$ [K]

$[PC_mLi^+\,C_n]^- + e^- + Li^+ \rightarrow C_3H_6 + Li_2CO_3 + nC + (1\text{-}m)PC$ [L]

A similar pathway for the decomposition of EC is proposed except that C_2H_4 is formed. Both the electrochemical-reduction and chemical-reduction steps results in the formation of a surface layer, which makes electron transfer more difficult and eventually leads to termination of gas

evolution. Analysis of the gas that is evolved from pressure measurements indicated that the amount of gas increased linearly as the voltage decreased to about 0.8 V, and below this voltage it starts to level off until about 0.2 V where gas formation ceases.

Various chemical approaches have been used to reduce the extent of electrolyte decomposition and irreversible capacity loss at the carbon negative electrode in Li-ion cells. One approach is to introduce chemical additives to the electrolyte that inhibit the electrolyte decomposition reactions. Besenhard *et al.* (89) observed that additives such as CO_2, N_2O, CO, CO-complexes and polysulfides S_x^{2-} in PC have a beneficial effect on the self-discharge and cycling behavior of lithiated carbon electrodes. These additives affect the film properties by decreasing the low-frequency impedance, and permitting more facile Li^+ ion transport. Furthermore, Besenhard and co-workers (90) reported that CO_2 in the nonaqueous electrolyte suppresses the co-intercalation of solvent molecules.

The addition of the crown ether, 12 crown 4, to nonaqueous electrolytes produced encouraging results in reducing the extent of electrolyte decomposition at carbon electrodes (87, 91-93). The role of 12 crown 4 is to suppress gas evolution and to aid in the formation of a more stable SEI layer (87,91). The addition of 12 crown 4 to 1 M $LiClO_4$ - PC/EC appears to restrict the second electron reduction of PC and EC, which forms propylene and ethylene (Reaction J). The addition of 0.1 M 12 crown 4 to the electrolyte reduced the voltage plateau at 0.8 V by 48% and the resulting electrolyte decomposition. The optimum effect was observed with an electrolyte containing about 0.35 M 12 crown 4. Shu and co-workers (94,95) also observed that an electrolyte containing chloroethylene carbonate and PC or PC-EC exhibited improved performance in Li-ion cells, which they attributed to reduced electrolyte decomposition and low self-discharge.

The surface morphology of carbon in negative electrodes also has a major influence on the extent of electrolyte decomposition in Li-ion cells (96-99). The edge-plane sites of graphite are observed to be more active for electrolyte decomposition than the basal-plane sites (98). Another approach to affect the amount of electrolyte decomposition is to modify the surface structure of graphite by oxidation (100-103). Peled *et al.* (99-101) reported that mild oxidation of graphite at 550°C for 1 h in air (6% burn-off) was found to improve its performance. The electrode degradation rate was much lower, reversible capacity increased by 10-30%, while the irreversible capacity loss decreased. These changes are attributed to the formation of a SEI layer that is chemically bonded to the surface carboxylic groups (>-COOH) at the zigzag (../\/\/\..) and armchair (../¯_/¯\..) faces, and to the presence of extra Li at the zigzag, armchair, and other edge sites and nanovoids.

4. CARBON ELECTRODES

4.1. Types of Carbons

Examples of the various types of precursors and carbonaceous materials that have been evaluated in negative electrodes for Li-ion cells are listed in Table 3 along with some of the companies which supplied the materials. This list is not all inclusive but is presented to illustrate the high level of activity that is occurring worldwide in the search for useful carbonaceous materials for Li-ion cells. Some of the important properties that affect the electrochemical behavior of carbons in Li-ion cells are crystallinity, surface area, type and amount of surface groups, particle size and shape. These parameters influence the capacity, cycling life, charge/discharge rate and energy efficiency. The properties are controlled by modifying the carbon precursor and processing conditions.

One of the many new carbons which have been considered for Li-ion cells are the so-called mesocarbon microbeads (MCMBs). The origin of MCMBs can be traced back to the observations by Brooks and Taylor (103b,103c) in the 1960's. They studied the carbonaceous mesophase that formed in the early stages of carbonization of pitches and proposed a model for the mesophase spherules, consisting of lamellar structure of oriented polycondensed aromatic hydrocarbons. During the heat treatment of pitches, spherules are formed which coalesce to become bulk mesophase, which is a step for the preparation of carbon materials by the liquid-phase carbonization of organic compounds. The term "mesophase" means "intermediate phase", and accordingly the carbonaceous mesophase is the intermediate material formed during carbonization of precursor materials to produce carbon. The historical development of the carbonaceous mesophase from which MCMBs are derived was reviewed by Honda (103d), who also named the mesophase spherules "mesocarbon microbeads".

The pyrolysis of pitches at temperatures between 350 and 500°C involves a mesophase transformation, during which. polycondensed aromatic hydrocarbons are formed by thermal decomposition and thermal polymerization reactions, followed by orientation of polycondensed aromatic hydrocarbons in a fixed direction. The mesophase spherule is formed by the accumulation of oriented polycondensed aromatic hydrocarbons in layers. When the spherules meet each other, coalescence occurs to produce larger droplets, leading eventually to bulk mesophase. The mesophase spherules can be separated from the pitch matrix by solvent fractionation. It is the heat-treated mesophase spherules which were obtained by Honda and co-workers using quinoline solvent extraction that they called mesocarbon microbeads. Other precursors such as coal tar, decant oil pitch and naphtha-tar pitch have been used to obtain MCMBs (103e). The MCMB from Osaka Gas that is listed in Table 3 originated from coal-tar pitch. The MCMB was separated from the coal-tar matrix by a high-temperature centrifugal separation and cleaned by washing with light oil to remove residual tar adhering to the MCMB surface. After drying, the MCMBs were classified so that the average particle size is about 6 μm. These particles were carbonized in nitrogen at temperatures from 700 to 1000°C, and then some of the samples were heat treated at various temperatures to 2800°C. MCMBs are "soft carbons" with a d(002)-spacing of 3.5 Å (heat treat at 1000°C), which decreased to 3.36 Å after heat treating at 2800°C to form a graphitic structure.

As noted in Table 3, many organic compounds have been used as precursors to obtain carbonaceous materials. One of the earlier studies on the thermal decomposition of polymers to obtain carbon negative electrodes for Li-ion cells was reported by Yamamoto *et al.* (103f). In general, the organic compounds are carbonized by heating at temperatures above 700°C in an inert environment (103f, 104-109). The hydrogen content (see Table 4), which is reported to play an important role in the Li storage capacity, varies with the heat-treatment temperature. The carbonaceous materials obtained at the lower temperatures (about 500°C) have a high hydrogen content, which decreases significantly to a H/C atomic ratio of less than 0.05 by heating to temperatures above about 1000°C. With many of the organic precursors such as the resins and polymeric materials, hard carbons (*e.g.,* glassy carbon) are formed which cannot be graphitized by high-temperature heat treatment. In the following section, the significance of hydrogen on the Li storage capacity is discussed.

4.2. Lithium Storage Mechanism

The characteristic properties of carbon materials and their influence on the mechanism by which Li is stored in the carbon are still subjects of much interest and debate. The insertion of Li ions between the graphite layer planes to form the classical intercalation compound represents only one of the proposed mechanism for Li storage in carbonaceous materials. The publications by Fischer and co-workers (12-35) provide an extensive discussion on Li intercalation of graphite. More recently, the rapid advances in the commercialization of Li-ion cells has led to a drive to increase the Li storage capacity of the negative electrode to beyond that for graphite,

namely 372 mAh/g. Correspondingly, new mechanisms to explain these high Li storage capacities >372 mAh/g have also been advanced.

Structure Considerations. Dahn and co-workers (110,111) undertook an extensive study of the correlation between Li insertion and the crystallographic structure of carbonaceous materials using X-ray diffraction (XRD) analysis. In their study, they utilized a parameter similar to the one that was defined by Franklin (112,113), which followed the original research on XRD of carbons by Warren (114-116). Franklin studied both non-graphitic and graphitic carbons, and concluded that the relative amounts of the disordered and ordered regions of the structure can be characterized by the parameter p, which is the proportion of disorganized layers ($p = 0$ for perfect graphite). Furthermore, she suggested that the d(002) spacing for the regions of organized layers is 3.354 Å, and that of the disorganized regions is 3.44 Å. The organized regions are considered to consist of crystalline domains that can be characterized by L_c and L_a, which are the crystallite sizes in the c-direction (perpendicular to the basal planes) and a-direction (parallel to the basal planes), respectively. On the other hand, the disorganized regions consist of highly strained domains of buckled graphite-like layer planes or groups of tetrahedrally bonded carbon. Following this early analysis, Dahn and co-workers developed a model based on the parameters g (fraction of organized regions) and P (probability of finding a random stacking shift between adjacent layers in the organized regions). Based on these definitions, $g = 0$ and $P = 1$ for disordered (amorphous) carbon, $g = 1$ and $P = 0$ for ordered (graphitic) carbon, and $g = 1$ and $P = 1$ for turbostratic (randomly stacked parallel layers) carbon. The physical model that can be derived from these parameters is: fraction of unorganized or buckled layers is proportional to $1-g$, probability of finding the rhombohedral-type stacked layers is P_t, and the probability of finding the hexagonal-type stacked layers is $1-P-P_t$. Dahn and co-workers developed a structure model that utilizes a computer program to analyze the XRD patterns of carbonaceous materials to obtain structural parameters. From their analysis they derived an expression

$$x_{max} = g\{(1 - P) + P\,x_r\} + (1 - g)x_{uc} \qquad [1]$$

which relates the variation of the reversible capacity with the structural parameters. In this expression x_{max} is the maximum reversible capacity, x_{uc} is the amount of Li per six carbon atoms that is reversibly intercalated in the unorganized regions (may be buckled single layers or highly strained layers), and x_r is the amount of Li per six carbon atoms that is reversibly intercalated in the turbostratic regions. With x_{uc} and x_r as adjustable parameters, the capacity for Li intercalation in over 40 cokes, carbon fibers, synthetic graphites and mesocarbon microbeads was successfully predicted.

Subsequently, Shi *et al.* (117) extended the original studies by Dahn and co-workers by more detailed analysis of the influence of the graphite crystal structure on Li intercalation. Specifically, they examined the distribution of hexagonal (2H) and rhombohedral (3R) contents of graphite by XRD and their role in the reversible Li intercalation capacity. In a typical graphite, the 2H structure dominates with layer planes arranged in the ABAB.... sequence. The 3R structure has layer planes arranged in the ABCABC.... sequence, with the C layers shifted by an equal distance as that for the A and B layer planes. Using the XRD peak intensity (I) for graphites, the fraction x of the 3R content can be determined by the relationship

$$I = (1 - x)I_{2H} + xI_{3R} \qquad [2]$$

where I_{2H} and I_{3R} are the XRD peak intensities for 2H and 3R graphites, respectively. From this analysis, a correlation was developed between the XRD peak intensities and the parameter P_{2H}, which is a measure of the turbostratic disorder in the graphite structure (also is related to the probability of finding a random stacking between any two adjacent layers). The reversible capacity (C_{rev}) is then a function of P_{2H},

$$C_{rev} = 372P_{2H}\,(mAh/g) \qquad [3]$$

A similar relationship is proposed for the 3R structure so that the total reversible capacity (C_t) is equal to the sum of the capacities of the two graphite structures,

$$C_t = 372x(1 - P_{3R}) + 372(1 - P_{2H}) \text{ (mAh/g)} \quad [4]$$

This correlation provides good agreement between the reversible capacities obtained experimentally and that obtained from Equation 4 which takes into account the relative fraction of the hexagonal and rhombohedral structures in graphite. Flandrois et al. (117b) described in their U.S. Patent an ultrasonic technique to produce >10% rhombohedral from conventional graphite. The irreversible capacity loss was lower in graphites which contained a higher fraction of the rhombohedral phase.

Dahn and co-workers (118-120a) suggested a mechanism to explain the high reversible Li storage capacity (*i.e.*, >450 mAh/g) of hard carbons. They suggested that these carbons, which are produced by carbonization of organic precursors such as epoxy novolak resins, have a structure which resemble a "house of cards" that consists of a significant fraction of single, bilayer, or trilayer graphene sheets arranged at arbitrary angles. Because of this random stacking, these carbons also contain micropores. Li can insert reversibly into these carbons, and the amount of Li that can be inserted increases as the fraction of single layers increases. This suggests that the mechanism of Li insertion involves surface adsorption of Li on the internal surface of the single layers of graphene sheets, and Li can be adsorbed on both sides of a single graphene layer. The conclusion from these studies is that the hard carbons which have the smallest fraction of parallel-stacked graphene layers and the largest number of nanoscopic pores per unit mass have the highest capacity for Li insertion. Following this proposed mechanism, Fischer and co-workers (120b) used neutron scattering techniques to analyze the composition and structure of epoxy novolak resins that were pyrolyzed at 650 and 1000°C. Their experimental results and computer simulations supported the model by Dahn (*i.e.*, house of cards) for pyrolyzed resins, with the carbon structure consisting of small graphene layer fragments with lateral dimensions of about 10 Å. In addition, the residual hydrogen is bonded to the edge sites on the carbon structure, and this hydrogen is involved in the mechanism for Li storage.

More recently, Dahn and co-workers (120c) extended their analysis of the house of cards model and presented a "falling card model." This model describes the change in the pore size and structure with changes in the processing conditions to form the amorphous carbon. X-ray diffraction (XRD) and small-angle X-ray scattering (SAXS) were used to derive the parameters R and R_g, respectively. The parameter R is defined as the ratio of the XRD peak height to the background signal. The parameter R_g is the radius of gyration obtained from SAXS which is a dimension characteristic of the pore size. Based on this analysis, Dahn and co-workers reported that the best carbons for Li-ion batteries are those that have the lowest values of R and R_g.

Cavity Mechanism. Disordered carbons have regions in the structure where small crystallite planes intersect in a random pattern (*i.e.*, one model is the house-of-cards structure). These regions may contain microcavities (voids) which could provide sites for storage of Li.

Mabuchi and co-workers (121-123) measured the Li storage capacity of mesocarbon microbeads (MCMB) and observed a high charge-discharge capacity of 750 mAh/g with MCMB that was heat treated at 700°C. This result suggested that another mechanism takes place, besides the well-known mechanism for Li intercalation between the layer planes, during the charge/discharge reaction in disordered carbons. To explain the high Li storage capacity of disordered carbons, Mabuchi and co-workers proposed that the interlayer spaces in MCMB are capable of storing excess Li species, as well as the cavities that may be present (cavity mechanism). A schematic representation of the insertion and de-insertion of Li during charge and discharge, respectively, is presented in Figure 7. In this model, Li ions occupy the region

between the layer planes, much like the arrangement found in Li-intercalated compound. In addition, the cavities present in the carbon are capable of storing additional Li. The Li species in the cavities reported to be Li-ion clusters which are capable of more close packing. This will permit a higher storage capacity of Li in the carbon sample than that if only Li was present between the layer planes.

The relationship between the structural parameters of carbons and the composition of lithiated carbons was examined by Mabuchi and co-workers (124,125) to derive a quantitative model to explain the results. In the case of graphite, a relationship was derived (124) that relates the ratio of Li to carbon that is intercalated (Li/C) to the crystallographic parameters, *i.e.*,

$$C/Li = 6\left(1 + d_{002}/L_c\right)\left(1 + 2d_{c\text{-}c}[\sqrt{3}L_a + d_{c\text{-}c}]/[L_a^2 + d_{c\text{-}c}^2]\right) \quad [5]$$

where $d_{c\text{-}c} = 1.42$ Å, and d(002), L_a and L_c are the crystallographic parameters for the interlayer spacing and crystallite size in the a- and c-direction, respectively. This analysis was extended to account for the presence of cavities in the microstructure of disordered carbons and the storage of Li in these cavities at potentials greater than about 0.9 V ("second region"). The total volume of the cavities of the disordered carbon relative to ideal graphite ($\int dV_{cav}$) is represented in terms of the structural parameters, *i.e.*,

$$\int dV_{cav} = \left(1 - \rho/\rho^\circ\right)\left(d_{002}/d_{002}^\circ\right)\left(d_{c\text{-}c}/d_{c\text{-}c}^\circ\right)\left(L_c/[1 + d_{002}]\right)\left(L_a/[L_a + d_{c\text{-}c}]\right)^2 \quad [6]$$

where ρ is the density, and the superscript, $^\circ$, denotes the parameters for ideal graphite. In the case of graphite, $\int dV_{cav} = 0$, whereas for MCMB obtained at 600°C, the corresponding $\int dV_{cav} = 0.55$. Mabuchi and co-workers observed a linear relationship between the discharge capacity at potentials in the second region and $\int dV_{cav}$, suggesting additional Li storage in the cavities. The capacity of Li in the cavity, Q_{cav}, is equal to

$$Q_{cav} = \left(\int dV_{cav}/\rho a_{Li}^3\right)(F/N) \quad [7]$$

where a_{Li} is the lattice constant for the bcc structure of Li, N is the Avogadro number, and F is the Faraday constant. Satisfactory agreement was obtained between the experimental capacities for Li storage and the theoretical capacities determined by Equation (7).

Surface Interactions. Surface sites and surface species associated with disordered carbons are capable of enhancing the Li-storage capacity of these carbons, according to the studies by several research groups. Dahn and co-workers (105,106,126) used organic precursors to prepare a series of disordered carbons which were found to have high hydrogen content (*e.g.*, see H/C ratios in Table 4). The Li-storage capacities obtained with these carbons were also high, up to 800 mAh/g. To explain these results, Dahn and co-workers proposed that Li binds to hydrogen that terminates the edge sites of the carbon layer planes, as represented in Figure 8. A strong correlation was found between the hydrogen content and the Li-storage capacity of carbon. Fischer and co-workers (127) substantiated the relationship between the hydrogen content of disordered carbons and their Li storage capacity. A semiempirical computer simulation was used which showed that the high capacity is partially connected to Li bonding to hydrogen on the edge sites of the carbon. More recently, Nakadaira *et al.* (128) also conducted a theoretical analysis of the high Li storage capacity of disordered carbons. A semiempirical calculation was used to determine the electronic structure of Li ions doped in a small graphite cluster with dangling bonds or hydrogen terminations at the edge. This study indicated that two sites for Li ions were available in the small graphitic clusters which are present in disordered carbons. These two sites have different chemical bonding which is identified with ionic ($Li^{+0.6e}$) and covalent ($Li^{+0.3e}$ - $Li^{+0.5e}$) bonds. The different ionicities are dependent on (i) the presence of hydrogen-terminated edges, (ii) the presence of dangling bonds at the edges, and (iii) bonding of Li ions at the edge to one or two carbon atoms. The researchers further propose that the

cluster edge surface plays a special role in accommodating excess Li ions in the disordered carbon structure.

Matsumura and co-workers (129,130) explained their high Li storage capacity of disordered carbons by proposing a mechanism that involves sites at the edges, crystallite surfaces, and between the layer planes. The interaction of Li and the edge sites associated with the small crystallite in disordered carbon is illustrated schematically in Figure 9. In this situation, the researchers suggest that the interaction between carbon and Li is similar to that in Li-doped polyacetylene. The availability of these three different sites in disordered carbons accounts for the high Li storage capacity. Mori *et al.* (131) suggested that two distinct sites for Li storage are available in the highly disordered carbons they prepared by heat treating pitch coke at 750°C and 1000°C in nitrogen. Li^7 NMR measurements suggested that two types of Li doping sites exist in the coke: one type (S-site) has a wide range of spinning side bands while the other (C-site) has a narrower range (see Figure 10). It is considered that C-site Li atoms are located between the carbon sheets, while S-site Li atoms are located at the surface of the microcrystallites formed by these sheets or at their microcavities. During charge, Li atoms enter between the layer planes to the C-sites, which appear similar to the sites for the conventional intercalation mechanism. At the same time and to a lesser extent, Li binds to the S-sites, which occurs later during charge. When the electrode is discharged, Li leaves the C-sites more readily, and the Li associated with the S-sites remaining until the later stages of discharge. The mechanisms proposed by the groups of Matsumura and Mori have strong similarities. In both cases, invoking the presence of surface sites at the edges of the disordered carbon crystallites which bind Li offers an explanation for the enhanced Li storage capacity.

Covalent Lithium. Sato *et al.* (132,133) utilized high-resolution transmission electron microscopy and Li^7 NMR measurements to study the high Li storage capacity (up to 1000 mAh/g) of disordered carbons obtained by heat treatment of polyphenylene. The NMR spectrum suggested the existence of Li_2 covalent molecules in the disordered carbon, and their location is indicated in the schematic representation in Figure 11. Two distinct sites for Li are indicated, one site (Site A) is for the ionic Li species which are typically found in intercalated carbon, and the other site (Site B) is occupied by covalent Li. The bond length of the Li-Li bond in covalent Li is 2.672 Å, which is only slightly longer than the distance between the centers of adjacent carbon hexagons (2.46 Å for graphite). The covalent Li bond distance is less than the corresponding Li-Li bond distance in metallic Li (3.032 Å). The covalent Li accounts for the high Li storage capacity of this disordered carbon. The close packing of the ionic and covalent Li in the carbon structure corresponds to a composition of LiC_2, which has been obtained by non-electrochemical methods (see discussion above). However, the composition LiC_2 was prepared from graphite and not a disordered carbon. However, LiC_2 was not stable under ambient pressure conditions. In this regard, the findings of Sato *et al.* represent a new development in the synthesis of lithiated carbonaceous materials.

4.3. Lithium Storage Capacity

Because of the large number of reports in the literature on the reversible capacity for Li storage in different carbonaceous materials, it is not practical to discuss each of the results in this review. Instead, only selected results from the literature are presented in Table 5 which illustrate the types of carbons, electrolytes and Li storage capacities which have been achieved. The results that are presented in Table 5 are arbitrarily divided according to the type of carbonaceous materials, ranging from graphite to highly disordered carbons such as those which are derived from polymer precursors or hydrocarbon sources. It is apparent from the results that the reversible Li storage capacity varies widely with different carbonaceous materials, from less than 372 mAh/g (LiC_6), which is typical for graphite, to much higher capacities with the disordered carbons derived from organic-based precursors (*e.g.*, polymers, sugar). In general, no attempt was made to differentiate between the different charge/discharge rates (*i.e.*, C-rate or current

density) which were used to obtain the reversible capacities. Using lower C-rates or lower current densities produce higher reversible capacities. For example, Wang et al. (134) obtained a reversible capacity of >600 mAh/g with carbon from pyrolyzed poly(p-phenylene) at a charge/discharge rate of 0.05 mA/cm^2, but at a higher current density of 0.35 mA/cm^2, the capacity decreased to <300 mAh/g. Other studies have also observed that the reversible capacity is also dependent on the de-intercalation rate of Li from graphite (141,150).

The results in Table 5 indicate that the intercalation of graphite is very sensitive to the electrolyte composition. With the appropriate liquid electrolyte, a reversible capacity of 372 mAh/g which corresponds to the limiting composition for graphite, LiC_6, is commonly obtained (80,135,139,150). With a polymer electrolyte, 340 mAh/g is obtained (135). After mechanical grinding, the reversible capacity of graphite increased to >372 mAh/g but the irreversible capacity loss also increased (147). Mild oxidation of graphite was also conducive to increasing the reversible capacity of graphite but the irreversible capacity loss increased with more extensive oxidation (101).

Coke exhibits reversible capacities that are typically close to 186 mAh/g or corresponding to a composition of LiC_{12} (6,80,151), but higher capacities have also been reported. For instance in liquid electrolytes, reversible capacities of 385 mAh/g (131), 450 mAh/g (142) and 394-589 mAh/g (120a), and 355 mAh/g in polymer electrolyte (157) were reported. The Li storage capacities of carbon fibers (169,170,173-182) and MCMB (173,175,204,205) are commonly in the range 200-250 mAh/g. However, >372 mAh/g has also been obtained with carbon fibers (142,143,162,183,184). In the case of MCMB, high reversible capacities, >400 mAh/g, were reported (206,145,147), but the pretreatment has a major impact on the irreversible capacity loss: 440 mAh/g after heat treatment at 700°C (206) and 328 mAh/g after mechanical grinding (147). A high reversible capacity of 330 mAh/g with carbon fibers (166) in a liquid electrolyte, and 355 mAh/g in a polymer electrolyte (144,157), was observed. A much lower reversible capacity, 190 mAh/g, was obtained with carbon black in a polymer electrolyte (144,157).

MCMBs are reported to have several benefits in negative electrodes for Li-ion cells which have attracted attention; these include their spherical which permit close-packing and resultant high density and low surface area which minimizes the side reactions during charge/discharge. Graphitized MCMB in liquid electrolytes has a Li storage capacity that is lower than the theoretical equivalent for LiC_6 (372 mAh/g C). However, results obtained with a polymer electrolyte at 100°C or after mechanical grinding indicate that higher Li storage capacities are possible. The MCMBs that are exposed to lower heat-treatment temperatures (≤1000°) yield Li storage capacities that are higher or even exceed 372 mAh/g.

Electrochemical measurements on carbons obtained by pyrolysis of organic/polymer materials or CVD of vapor species show that elements such as boron, nitrogen, silicon, hydrogen and phosphorus can alter the Li storage capacity. The reversible capacities of these carbonaceous materials increased with the concentration of boron (192,208), hydrogen (104-106,188), phosphorus (190,195) and silicon (198,211,212). On the other hand the irreversible capacity loss increased with nitrogen content (210).

The potential-composition profiles in Figures 5 and 6 show that electrolyte decomposition and irreversible capacity loss occur in the first charge/discharge cycle. In subsequent cycles, the insertion and de-insertion of Li in the carbon structure dominates and represents the reversible capacity, with electrolyte decomposition occurring to a lesser extent. The relative magnitudes of the reversible capacity and the irreversible capacity loss are strong functions of the type and structure of the carbonaceous materials, as well as the composition of the nonaqueous electrolyte. The reversible capacity, irreversible capacity loss and the initial charge/discharge efficiency (Q_{rev}/Q_t) of pitch coke and natural graphite are functions of the type of carbonaceous

material and electrolyte, as illustrated in Table 6 (148). The electrolytes consisted of $LiPF_6$ and mixed solvents of propylene carbonate (PC), ethylene carbonate (PC), butylene carbonate (BC), 1,2-diethyl carbonate (DEC), γ-butyrolactone (γ-BL) and sulforan (SL). The results obtained with coke electrodes are essentially independent of the electrolyte, with reversible capacities of between 244-248 mAh/g and an irreversible capacity loss of about 57 mAh/g. On the other hand, graphite electrodes are clearly very sensitive to the electrolyte that is used, with gas evolution evident in PC/DEC and BC/DEC preventing Li intercalation. Furthermore, gas evolution results in degradation of the graphite structure. In SL/DEC and γ-BL/DEC, Li intercalation occurs but cannot be de-intercalated. Reversible intercalation with a capacity equivalent to LiC_6 was observed only in EC/DEC.

The decomposition of PC during the first intercalation/de-intercalation cycle is responsible for the poor electrochemical behavior of graphite in PC-containing electrolytes. However, by reducing the amount of PC in the mixed electrolyte (with $LiPF_6$), Nakamura *et al.* (215) were able to suppress electrolyte decomposition on graphitized MCMB. In PC/DEC (1:1) a irreversible capacity loss of 830 mAh/g was obtained, while in the 1:4 mixture, it was reduced to less than 100 mAh/g. Similar behavior was observed by reducing the amount of PC in electrolytes containing PC/MEC (methyl ethyl carbonate)and PC/DMC (dimethyl carbonate). For instance, a reversible capacity of 280 mAh/g and an irreversible capacity loss of 45 mAh/g were obtained in these two electrolytes with a 1:5 volume mixture, but electrolyte decomposition dominated in the 1:1 electrolyte mixtures. EinEli *et al.* (216) also concluded that MEC is a promising solvent for rechargeable Li-ion cells.

From the above discussion, it is apparent that the magnitude of the reversible Li storage capacity (Q_{rev}) is strongly dependent on many parameters, including the physical properties of the carbon, electrolyte composition, current density and the potential range over which intercalation/deintercalation takes place (see Tables 5 and 6). Furthermore, the discussion in the preceding section summarized several different mechanisms that have been proposed to explain the high Li storage capacities obtained with disordered carbons. Several researchers have presented a more simplified relationship between the crystallographic structure of carbon and its reversible Li storage capacity. One such correlation is the change in Q_{rev} with d(002) spacing (204,217,218). Published data for Q_{rev} obtained with various carbonaceous materials, ranging from highly ordered graphite to highly disordered carbon, are plotted as a function of their d(002) spacing in Figure 12. In this plot, no attempt was made to differentiate between the methods used to obtain Q_{rev}. Furthermore, the plot does not indicate the source of the data, but different symbols are used to indicate the various sources that are cited. It should be pointed out, however, that data from many of the major research organizations that have published results for Q_{rev} are included in the plot. A solid line is shown on the plot to illustrate a trend in Q_{rev} as a function of the d(002) spacing. Based on this line, there appears to be a minimum in Q_{rev} at a d(002) spacing of approximately 3.44 Å. Perhaps coincidentally, the degree of graphitization G is equal to zero at d(002) = 3.44 Å, according to Maire and Mering (219), *i.e.*,

$$G = \frac{[d(002) - 3.44]}{[M]}/(-0.086)$$

For d(002) of 3.44 Å --> 3.354 Å, G changes from 0 --> 1, and at d(002) = 3.44 Å, carbon is turbostratic. Taking the result in Figure 12, and the degree of graphitization derived by Maire and Mering, we suggest that the ability of carbonaceous materials to intercalate Li decreases as G --> 0 and d(002) --> 3.44 Å because the structure becomes turbostratic. However, for d(002) > 3.44 Å, the crystallite domains L_a and L_{ac} become smaller, microcavities are present, and the probability of forming single graphene planes increase. Under these conditions, Li insertion by the mechanisms discussed above can occur and account for the increase in x (see Figure 12). This analysis provides one simplified explanation for the experimental results in Figure 12 but it has not been verified.

5. ALTERNATIVE NEGATIVE ELECTRODE MATERIALS

A wide range of carbonaceous materials has been considered for commercial Li-ion cells, as noted by the list in Table 3. The amount of Li that can be stored efficiently in carbon is strongly dependent on the type of carbon, ranging from about $x = 0.5$ in petroleum coke, $x = 1$ in graphite to $x > 1$ in some amorphous carbons (x in Li_xC_6). In addition to carbon, attention has been focused on Li alloys and lithiated metal oxides as alternative negative electrodes for Li-ion cells. Some of the requirements for an alternative to carbon for the negative electrode in Li-ion cells, which rely on intercalation or insertion of Li ions in the host structure, include (i) low equivalent weight, (ii) small change in free energy for the Li insertion reaction, (iii) high reversibility for Li ion insertion/de-insertion, (iv) high Li-ion diffusivity in the host structure, (v) good electronic conductivity, (vi) thermal and chemical stability toward the electrolyte, and (vii) ease of fabrication into suitable electrode structures.

5.1. Alloys

The early work by Dey (220) demonstrating that Li forms alloys with a wide range of metals in nonaqueous liquid electrolytes initiated other investigations of Li alloys as an alternative to metallic Li for Li batteries. An excellent summary on alternative electrode materials to metallic Li, which includes metal-based electrodes and polymer-based electrodes for negative electrodes, is presented by Fauteux and Koksbang (221). The reversible insertion of Li in metal/alloys has been studied extensively because of their application in high-temperature molten salt Li cells. The following reaction is representative of the electrochemical reactions that occur during discharge of a Li alloy electrode:

$$Li_xM \rightarrow Li_yM + Li^+ + e^- \qquad [N]$$

where M = Al or Si, and Li_xM and Li_yM represent two solid phases in equilibrium. Besides Al and Si, other suitable alloying elements for Li are Sn, Pb, Bi, Sb and As. Taking the example of Li-Al and Li-Si alloys, their specific capacities are 610 mAh/g for electrodes cycled between 10 at% ($Li_{0.111}Al$) and 47 at% ($Li_{0.887}Al$) and 1440 mAh/g for electrodes cycled between 50 at% and 80 at%, respectively. These specific capacities are considerably higher than that of lithiated graphite, LiC_6, and therefore, are attractive alternatives to carbon-based negative electrodes. In addition, the penalty for reduced potential relative to metallic Li is acceptable, amounting to about 0.36 V for Li-Al and 0.2 V for $Li_{4.4}Si$. For comparison, Fauteux and Koksbang suggest that the penalty for lithiated graphite is 0.5 V.

One major problem with Li alloys in negative electrodes is the rapid disintegration of their mechanical structure upon repeated charge/discharge cycling in Li cells (221,222). A large volume change occurs during charge/discharge cycling as Li in introduced or removed from the Li alloy, and a concomitant deterioration of the alloy structure occurs. To stabilize the structure, small particles of Li alloys were embedded in a matrix or a second metal was incorporated in the structure with the Li alloy (*e.g.*, LiAl + Al_3Ni). Yang *et al.* (223) demonstrated an impressive improvement in the cycling performance of Li-alloy electrodes ($M + xLi^+ + xe^- <--> Li_xM$) in rechargeable Li cells by replacing the compact or large particle size metallic host matrices M (*e.g.*, Sn or Sb) with a small particle size (micro- or nano-scale) multiphase metallic host material like $Sn/SnSb_n$ or $Sn/SnAg_n$. The small particles expand to form a porous material, but without producing major cracks, during the first Li insertion. This behavior may be related to the small absolute changes in the size of the individual particles, and also with the fact that the more reactive particles are allowed to expand in a soft and ductile surrounding of still unreacted material.

5.2. Metal Oxides

Recently, tin oxide compounds were reported to be an attractive alternative material to carbon for the negative electrode in Li-ion cells. The Fuji Photo Film Co., Ltd. in Japan announced the development of Li-ion cells based on tin oxide compounds (224). They announced that a new company responsible for development, production and sales of the new Li-ion cell will be formed for volume production of a cylindrical cell which offers 50% more capacity than conventional carbon in Li-ion cells. The newly developed amorphous material for the negative electrode, which is a tin-based composite oxide, is reported to offer a number of advantages over the carbon conventionally used in Li-ion cells, such as: (i) theoretical volume capacity of 3,200 mAh/cm^3, four times that of graphite (*i.e.*, 837 mAh/cm^3), (ii) theoretical specific capacity of 800 mAh/g, twice that of graphite (*i.e.*, 372 mAh/g), and (iii) enhanced safety because the Li is in a highly ionized state. In addition, a cycle life of about 500 cycles was reported (224).

Dahn (225) examined the electrochemical behavior of a variety of Sn-containing compounds (*e.g.*, Sn, SnO, SnO_2, Li_2SnO_3, $SiSnO_3$ glass) for Li storage in $LiPF_6$/EC+DEC. Charge/discharge cycling of electrodes containing tin compounds, combined with *in situ* XRD analysis were used to understand the electrochemical behavior of the electrodes. The electrochemical behavior that takes place during cycling can be illustrated by the following series of reactions:

$$Sn + 4.4\,Li \rightarrow Li_{4.4}Sn \qquad [O]$$

$$SnO + 6.4Li \rightarrow Li_{4.4}Sn + Li_2O \qquad [P]$$

$$SnO_2 + 8.4Li \rightarrow Li_{4.4}Sn + 2Li_2O \qquad [Q]$$

$$Li_2SnO_3 + 8.4Li \rightarrow Li_{4.4}Sn + 3Li_2O \qquad [R]$$

$$SiSnO_3 + 6.4Li \rightarrow Li_{4.4}Sn + Li_2O + SiO_2O \qquad [S]$$

Upon reversal of the current (discharge), the Li-Sn alloy reacts (de-alloy) reversibly while the other compounds remain essentially unchanged:

$$\text{Li-Sn alloy} \rightarrow Sn + Li \qquad [T]$$

Dahn concluded that a Li-Sn alloy was eventually formed during charge/discharge cycling, which may be dispersed in a matrix containing Li_2O. The net result may be that a dispersed alloy of Li-Sn serves as the host for the charge/discharge of Li. The Li storage capacity of $Li_{4.4}Sn$ is equivalent to 790 mAh/g, which would provide a clear advance over that of graphite (*i.e.*, 372 mAh/g). However, the irreversible capacity is significant (200-700 mAh/g).

More recently, Fuji Photo Film Co., Ltd. (226) disclosed some details on their tin-based amorphous composites. This material has a basic formula SnM_xO_y ($x \geq 1$) where M is an element that is capable of forming a glass and which typically includes B(III), P(V) and Al(III). The oxide structure contains Sn(II)-O as the active centers for Li insertion, while the other elements serve to form the inactive network of -(M-O)- bonds. One synthesis procedure involves heating a powder mixture of SnO, B_2O_3, $Sn_2P_2O_7$ and Al_2O_3 (Sn:B:P:Al = 1.0:0.6:0.4:0.4 molar ratio) at 1100°C for 10 h. The resulting oxide, which has a composition $Sn_{1.0}B_{0.56}P_{0.4}Al_{0.42}O_{3.6}$ (designated TCO-1), has a density of 3.70 g/cm^3 and a surface area of 0.6 m^2/g after grinding to a powder. The charge (insertion)/discharge (de-insertion) of TCO-1 in 1 M $LiPF_6$/EC-DEC indicated 1030 mAh/g (first charge) and 650 mAh/g (first discharge), which is obtained in subsequent cycles and represents the reversible storage capacity. The irreversible capacity loss of 380 mAh/g (1030 mAh/g - 650 mAh/g) is attributed to an increase in resistance of TCO-1 during discharge. Other tin-based amorphous composites with molar compositions of Sn:B:P:Al = 1.0:0.4:0.4:0.3, 1.0:0.5:0.5:0.4, 1.0:0.6:0.5:0.1 and 1.0:0.5:0.4:0.1 have also

been prepared and showed capacities that were dependent on the Sn (II) content. It was observed that composites which did not contain Sn yielded essentially zero capacity.

The Li^7 NMR measurements by Idota *et al.* (226) indicate that a high ionic state of Li is retained in the charged state of TCO-1, as indicated by the chemical shift of 10 ppm (parts per million) for Li/Sn = 8. Their NMR studies (chemical shift of 16 ppm for Li/Sn = 4) further showed that crystalline SnO and Sn tend to form metallic Li similar to that found in a Li-Sn alloy. This latter observation corroborates the findings by Dahn (225).

Tin oxide is one of the metal oxides which has been evaluated for electrochromic applications. The electrochromic effect occurs by insertion and de-insertion of small cations such as Li^+. The observations from these studies are useful for understanding the role of tin oxide as a negative electrode material in Li-ion cells. Isidorsson and co-workers (227-229) prepared thin tin oxide films, Li_xSnO_2, by reactive rf magnetron sputtering of Sn, followed by electrochemical post-treatment. They suggested that the lithiation of SnO_2 in propylene carbonate with 1 M $LiClO_4$ is represented by the reaction

$$SnO_2 + xLi^+ + e^- \rightarrow Li_xSnO_2 \qquad [U]$$

The potential-composition (x in Li_xSnO_2) profile during lithiation showed evidence for two potential plateaus as the potential decreases initially from ~3.5 V; the first occurring at about 2 V (*vs.* Li) for $0.05 < x < 0.09$, and the second at about 1.2 V for $x > 0.12$. The potential drop at $x \sim 0.1$ is attributed to the transition of $Sn^{4+} \rightarrow Sn^{2+}$, which was detected by Mössbauer spectroscopy. Tin oxide films were prepared by Olivi *et al.* (230) and Orel *et al.* (231) using a dip-coat process [thermal decomposition of a tin citrate or tin chloride coated on a indium tin oxide (ITO) coated glass]. Reversible insertion/de-insertion of Li from tin oxide in nonaqueous electrolyte was reported. Orel *et al.* concluded that nanocrystallites (40 to 70 Å) of SnO_2 facilitate the reversible insertion/de-insertion of Li. However, Olivi *et al.* obtained reversible insertion/de-insertion of Li in crystalline SnO_2, although no observations were reported for an electrode that was cycled. These studies on thin-film electrodes suggest that the structure of SnO_2 is an important parameter, which could influence the reversible insertion/de-insertion of Li in Li-ion cells. Information provided by the Fuji Photo Film Co., Ltd. (224,226) indicated that an amorphous tin-based composite oxide was used as the negative electrode in Li-ion cells. The use of dopants and/or other additives in an amorphous structure are clearly beneficial for reversible insertion/de-insertion of Li.

The XRD results obtained by Dahn (225) indicate that Li-Sn alloys are formed by charge/discharge cycling of crystalline tin compounds in nonaqueous electrolytes. On the other hand, it appears that amorphous tin oxides, such as those used by Fuji Photo Film, and the thin-film materials used in the electrochromic applications are capable of cycling to form stable intercalation compounds. The amorphous structure may be the key to insuring reversible insertion/de-insertion of Li without converting to metallic tin and then to Li-Sn alloys, as observed by Dahn and co-workers.

Other examples of metal oxides which have been proposed as negative electrode materials for Li storage are iron oxide (232), vanadium oxide (233), and $TiO(OH)(H_2PO_4)$ (234). The high theoretical specific capacity (*i.e.*, 1000 mAh/g) and the availability of this capacity at <1 V are attractive features of lithiated iron oxide ($Li_6Fe_2O_3$). Amorphous Fe_2O_3-based thin-films were prepared by sputter-deposition by Sarradin *et al.* (232) and the reversible exchange of Li ions was investigated. The thin film electrodes were cycled in $LiAsF_6$/PC at the C/2 rate to 100% depth-of-discharge (DOD), and the Li storage capacity remained almost constant at close to 330 mAh/g after more than 120 cycles. Several hundreds of cycles were obtained by Sigala (233) with Li_8NiVO_4, and its capacity was about 600 mAh/g after 100 cycles (*i.e.*, >50% higher than the capacity obtained with graphite). Other compounds have been suggested as negative

electrodes for low-voltage Li cells. For example, Ferg *et al.* (235) proposed the use of $Li_4Ti_5O_{12}$, $Li_4Mn_5O_{12}$ and $Li_2Mn_4O_9$ with a spinel-type structure as negative electrodes in rocking chair cells with cell voltages of 1.2 or 2.5 V, depending on the positive electrode. Nishijima *et al.* (236) reported that $Li_{3-x}Co_xN$ ($0 \leq x \leq 0.5$) showed good reversibility, high capacity (480 mAh/g) and low voltage, making it suitable for the negative electrode in secondary Li cells.

Besides the review by Fauteux and Koksbang (221), interested readers are referred to the review by Yazami and Munshi (237) for additional details on novel anode (negative) electrode materials for rechargeable Li batteries. They describe experimental results obtained on Li alloys, lithiated metal oxides and metal-doped carbon materials.

6. CONCLUDING REMARKS

An overview of the physicochemical and electrochemical properties of lithiated carbons for Li-ion cells is presented in this review. The discovery of Li-intercalated carbons occurred only in the middle of the 20th century, and investigations of this material for use in electrodes took place in the 1980s. Within a very short time span, commercial Li-ion cells with carbon in the negative electrodes were introduced into portable electronic devices. The remarkable progress that has taken place with Li-ion technology can be attributed in part to the proliferation of portable electronic devices such as camcorders, personal computers, cellular phones, etc., and their need for high-performance batteries. The worldwide effort on developing carbonaceous materials for Li-ion cells has been strong, and the net result is that a wide range of carbons, from highly disordered to well crystalline graphite, has been considered for Li-ion cells. However, graphitic carbons still remain the most widely used material in the negative electrode of Li-ion cells. More recently, alternative materials for the negative electrode in Li-ion cells were identified, most notably amorphous tin oxide by Fuji Photo Film Co., Ltd. in Japan. The impact that this alternative electrode material will have in displacing carbonaceous materials from Li-ion cells is not clear at this time. However, research on carbons and other compounds for negative electrodes in Li-ion cells is still likely to remain active for the foreseeable future.

ACKNOWLEDGMENT

This work was sponsored by the Assistant Secretary for Energy Efficiency and Renewable Energy, Office of Transportation Technologies, Office of Advanced Automotive Technologies and the Director, Office of Energy Research, Office of Basic Energy Sciences, Chemical Sciences Division of the U.S. Department of Energy under Contract No. DE-AC03-76SF00098.

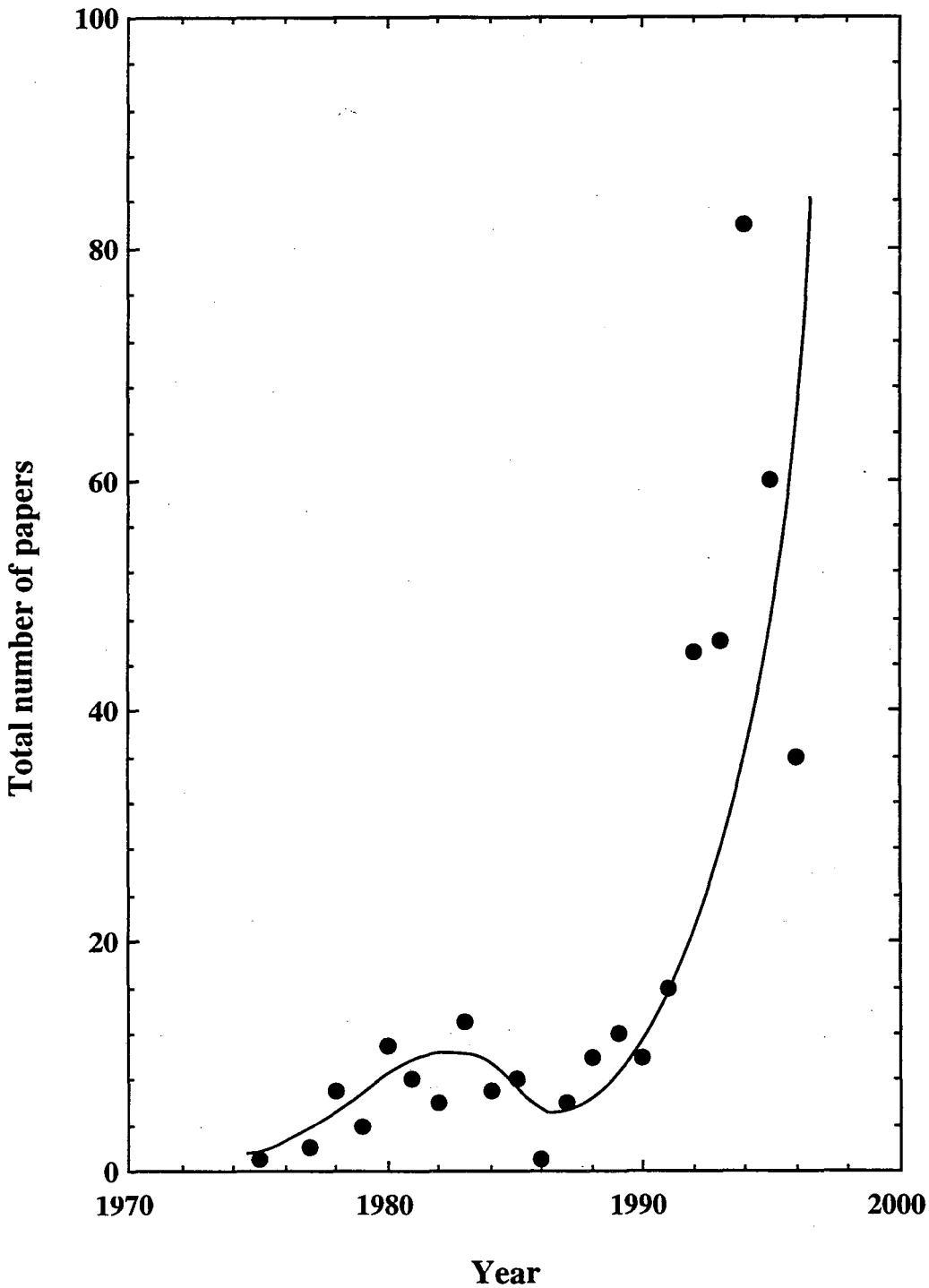

Figure 1. Number of technical publications on Li-intercalated carbon during the period 1975 to 1996.

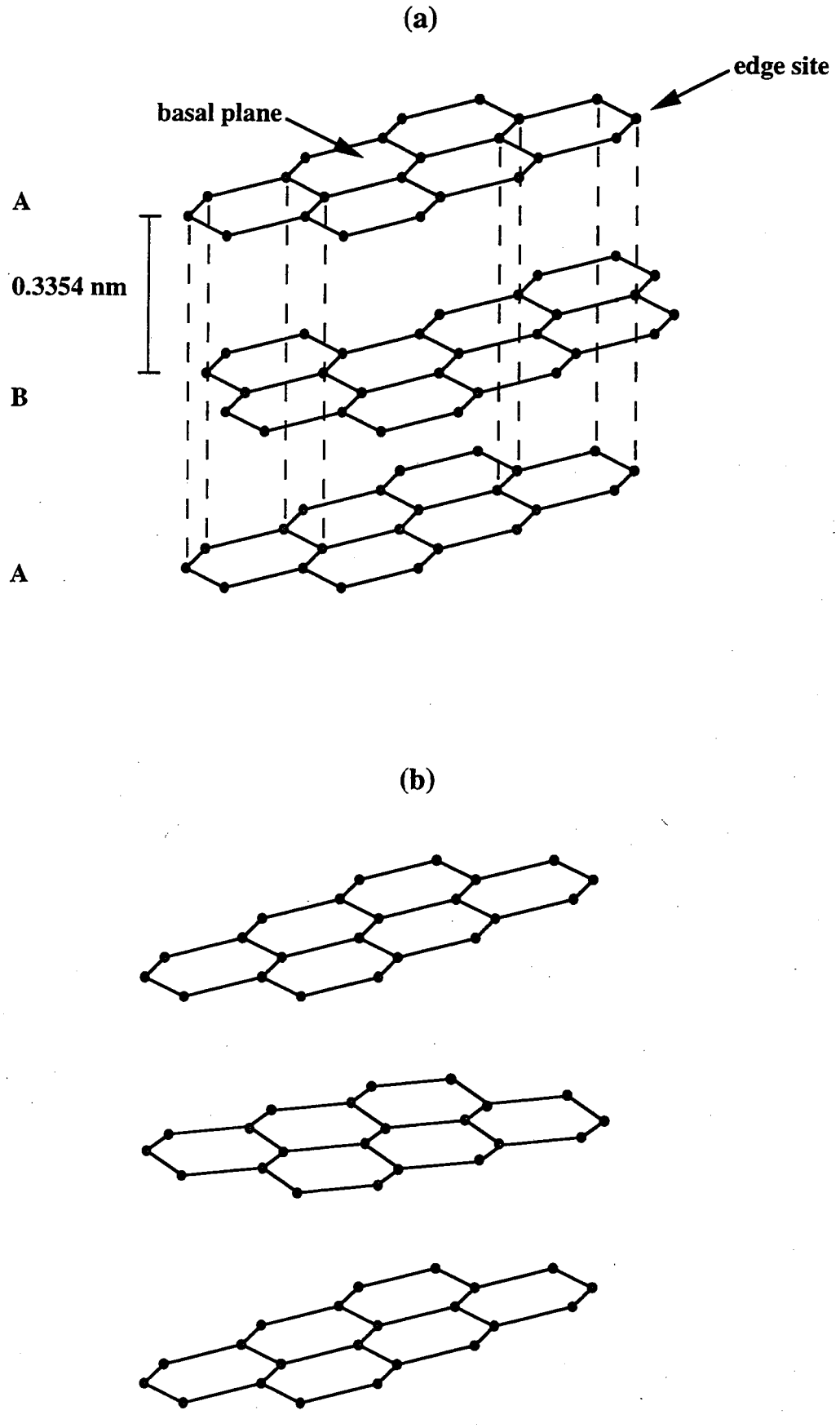

Figure 2. Crystallographic structure of graphite and amorphous carbon.

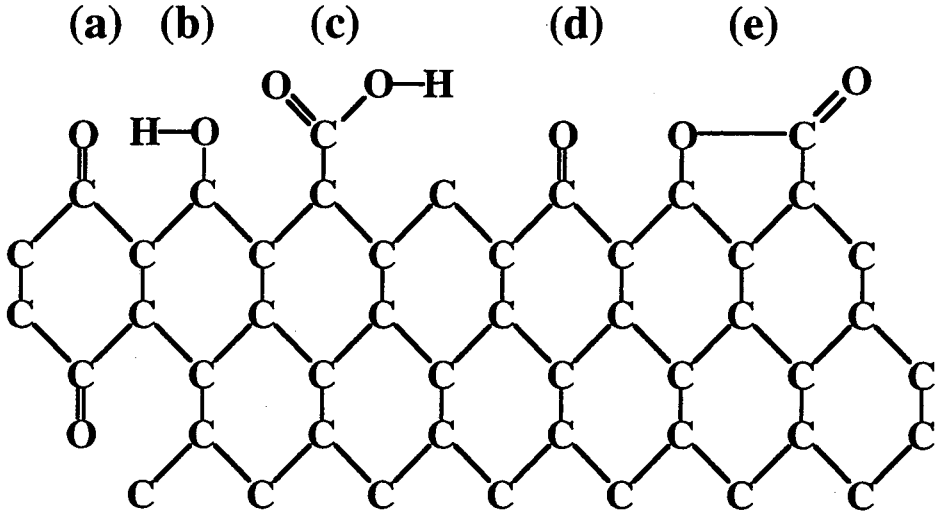

Figure 3. Schematic representation of oxygen-containing surface groups on carbon edge sites. (a) quinone, (b) phenol, (c) carboxyl, (d) carbonyl, (e) lactone.

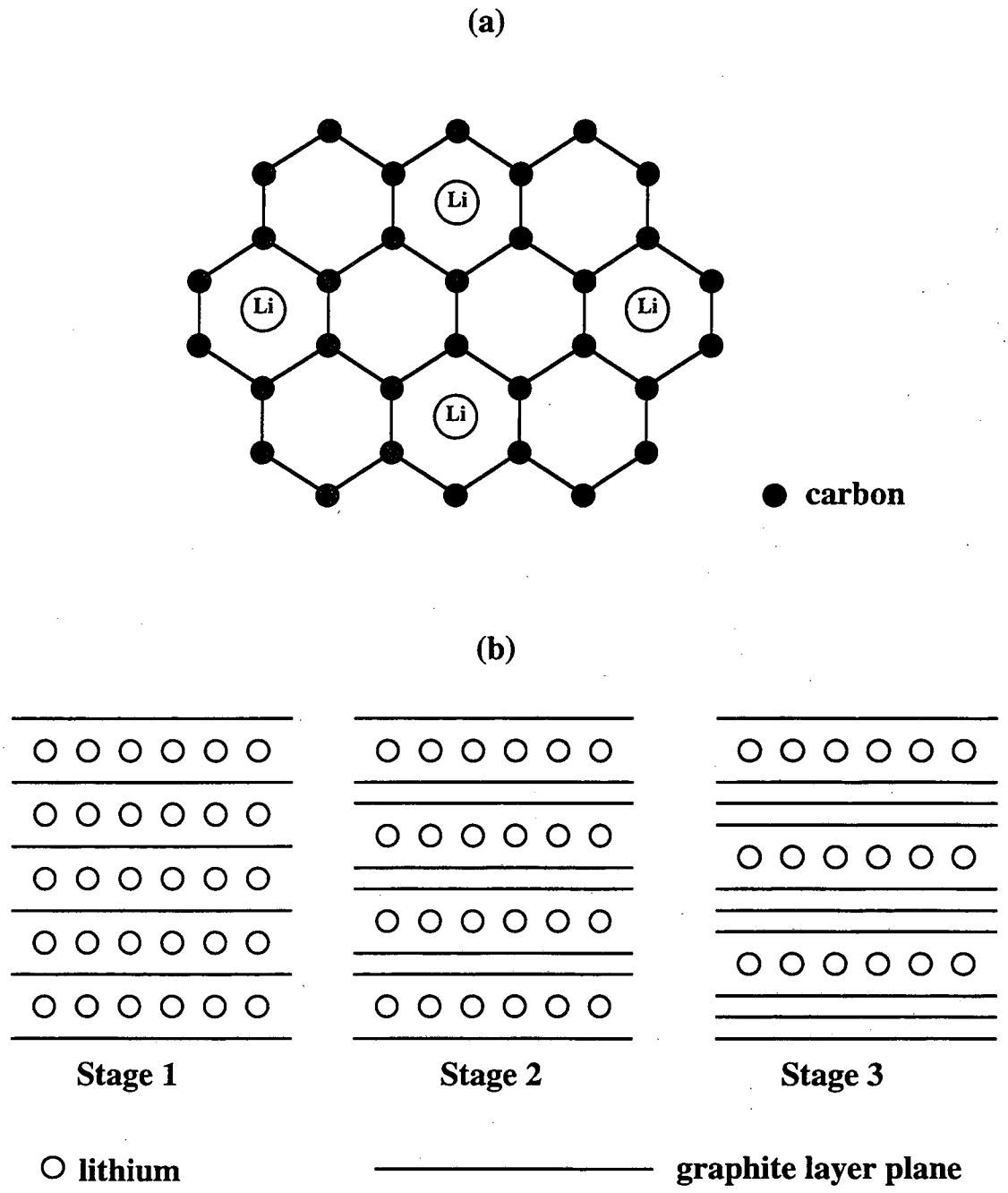

Figure 4. Schematic representation of the (a) arrangement of Li and carbon atoms in LiC_6, (b) layer structure of different stage compounds and (c) arrangement of Li and carbon atoms in LiC_4 and LiC_2.

(c)

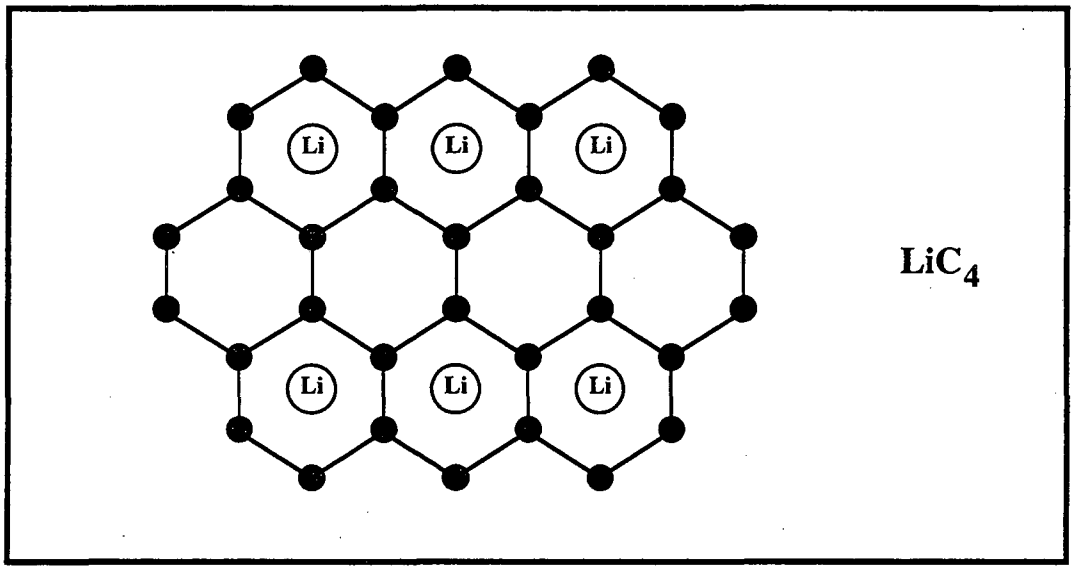

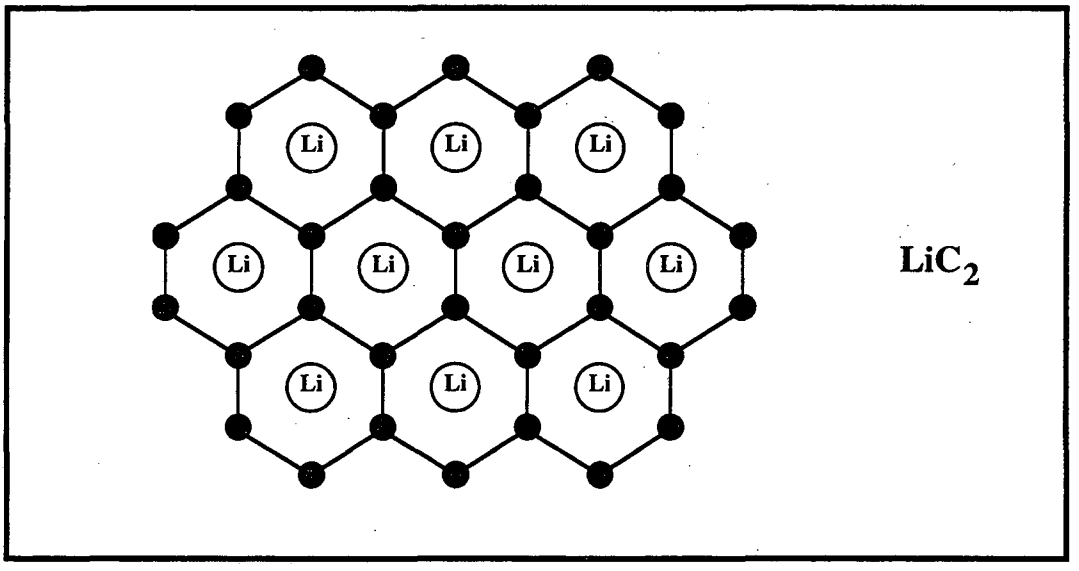

Figure 4

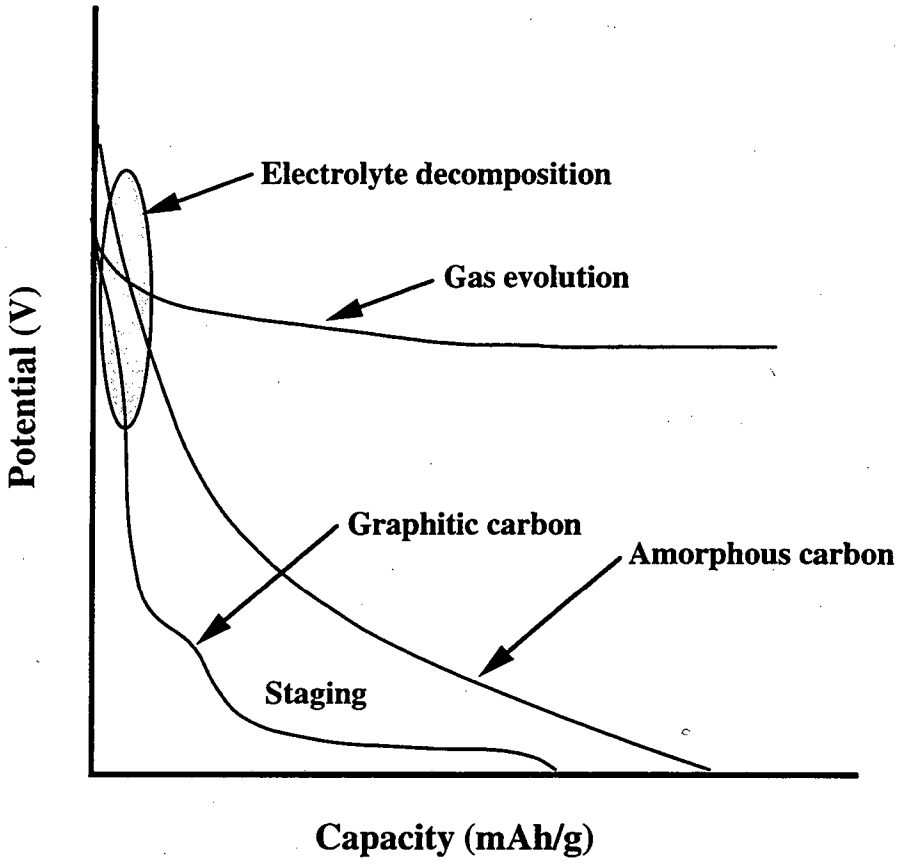

Figure 5. Schematic representation of the potential-composition profile for lithium intercalation of carbon electrodes.

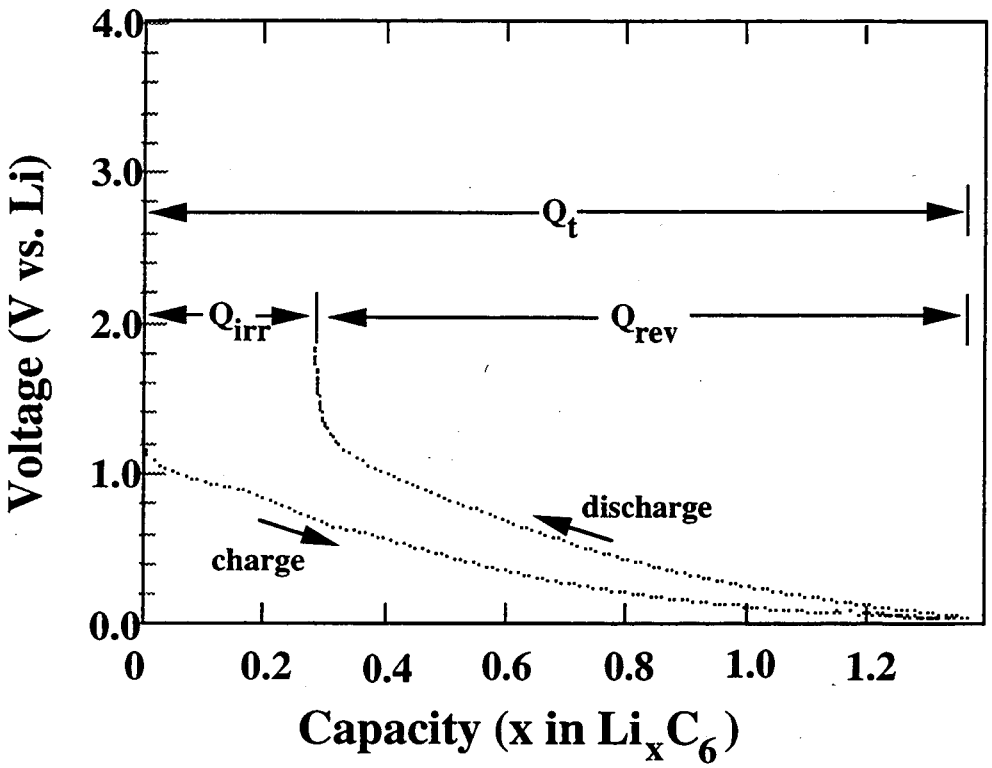

Figure 6. First charge/discharge cycle for amorphous carbon (unpublished data).

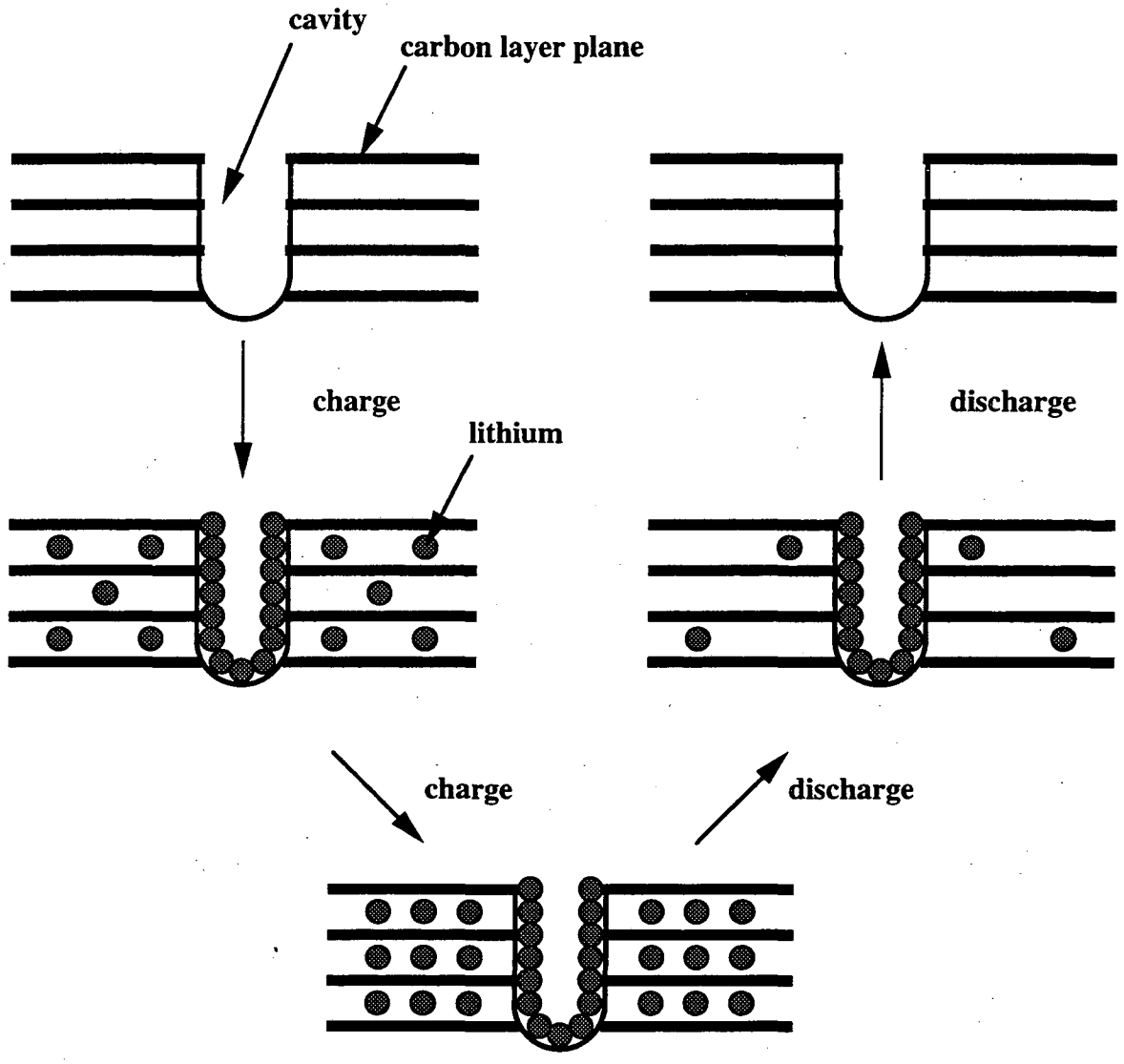

Figure 7. Schematic representation to illustrate the insertion and de-insertion of Li from highly disordered carbons which contain cavities.

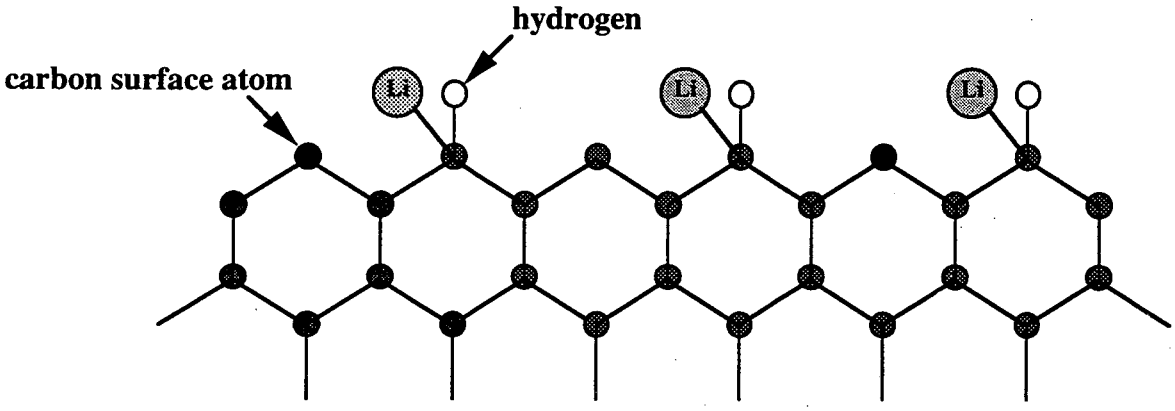

Figure 8. Schematic representation of bonding of Li and hydrogen in disordered carbons. Based on proposal by Dahn and co-workers (105, 106, 126).

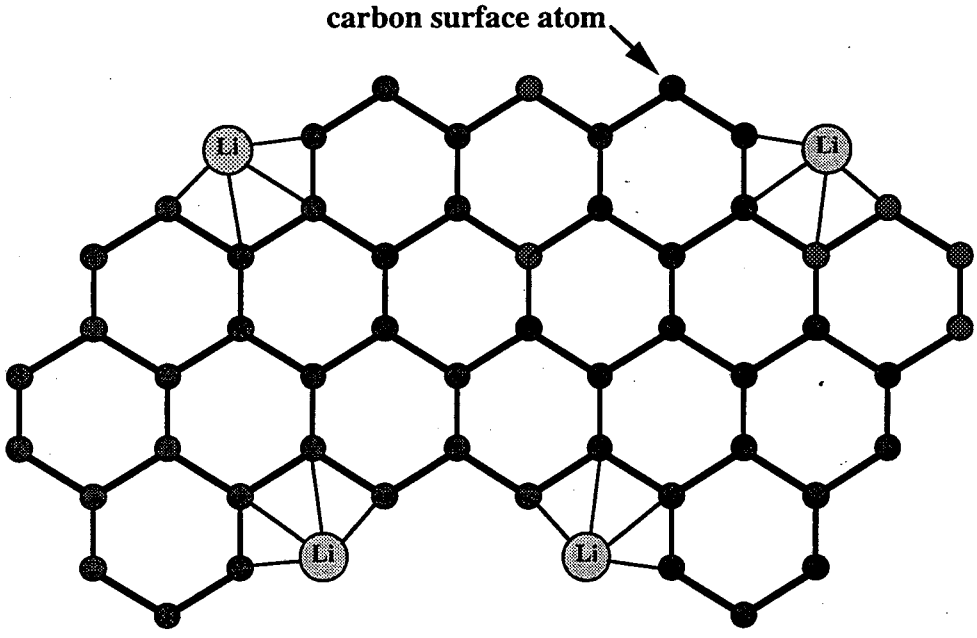

Figure 9. Schematic representation of bonding of Li and edge sites associated with small crystallites in disordered carbons. Based on proposal by Matsumura and co-workers (129, 130).

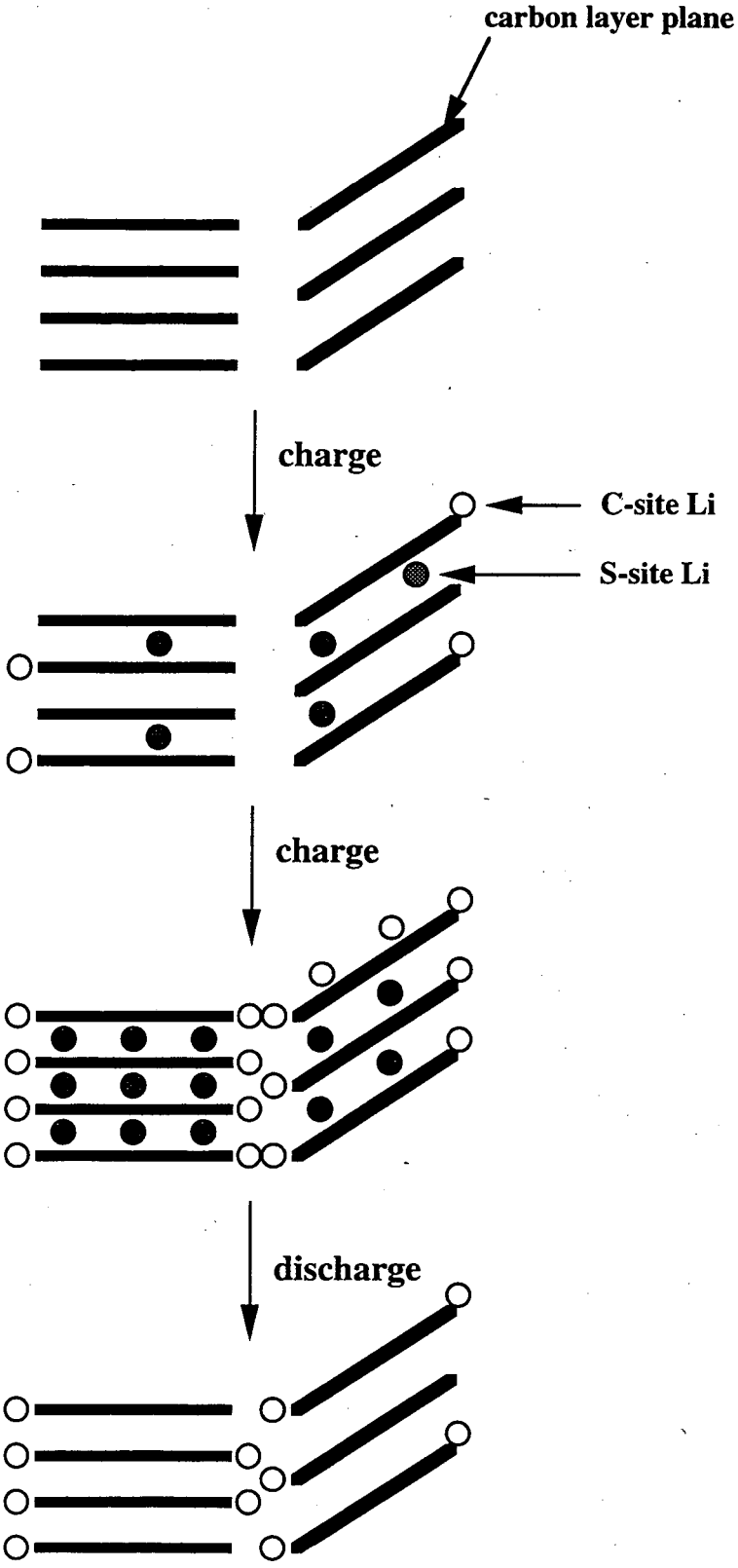

Figure 10. Schematic representation of C- and S- sites in disordered carbons, and Li storage with charge/discharge. Based on proposal by Mori and co-workers (131).

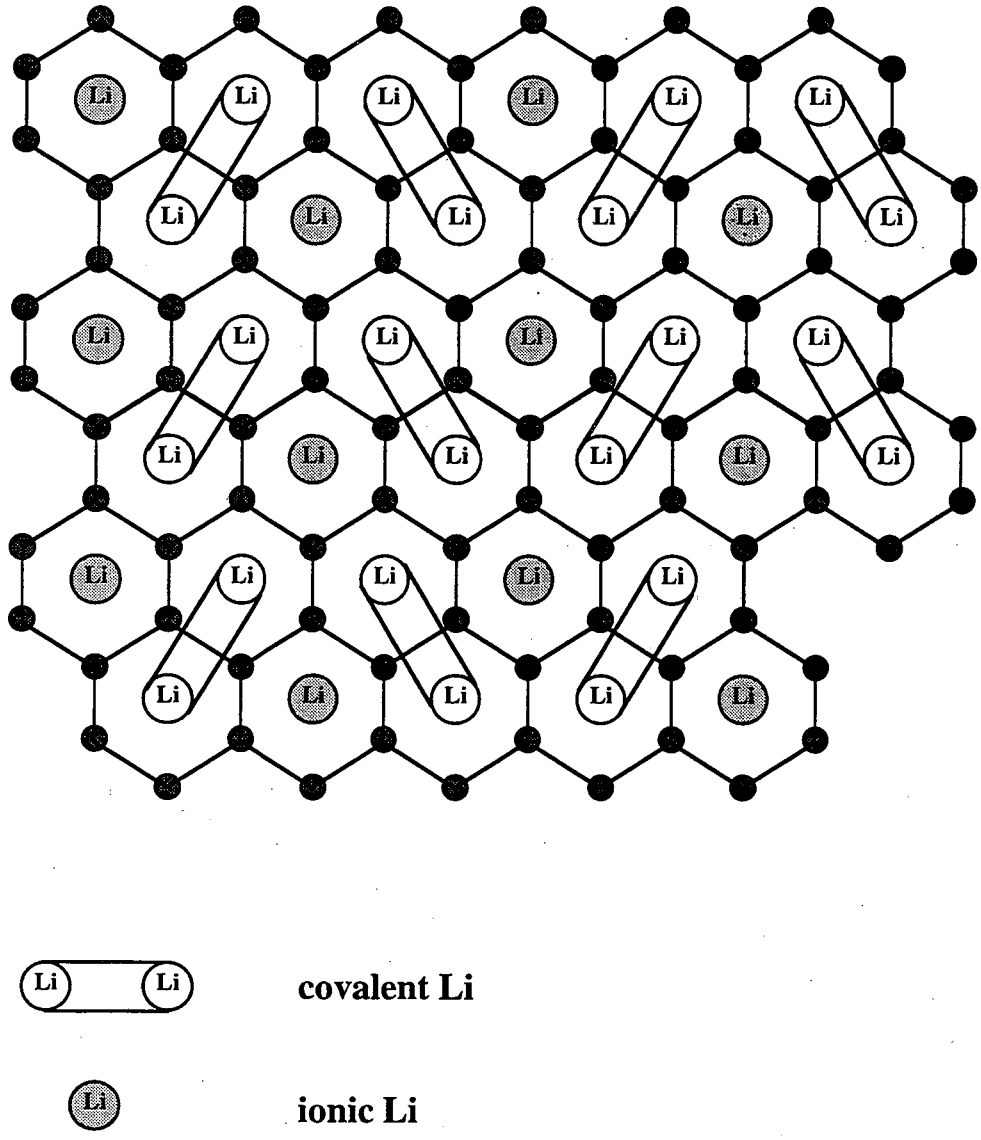

Figure 11. Schematic representation of covalent Li in disordered carbons. Based on proposal by Sato and co-workers (132, 133).

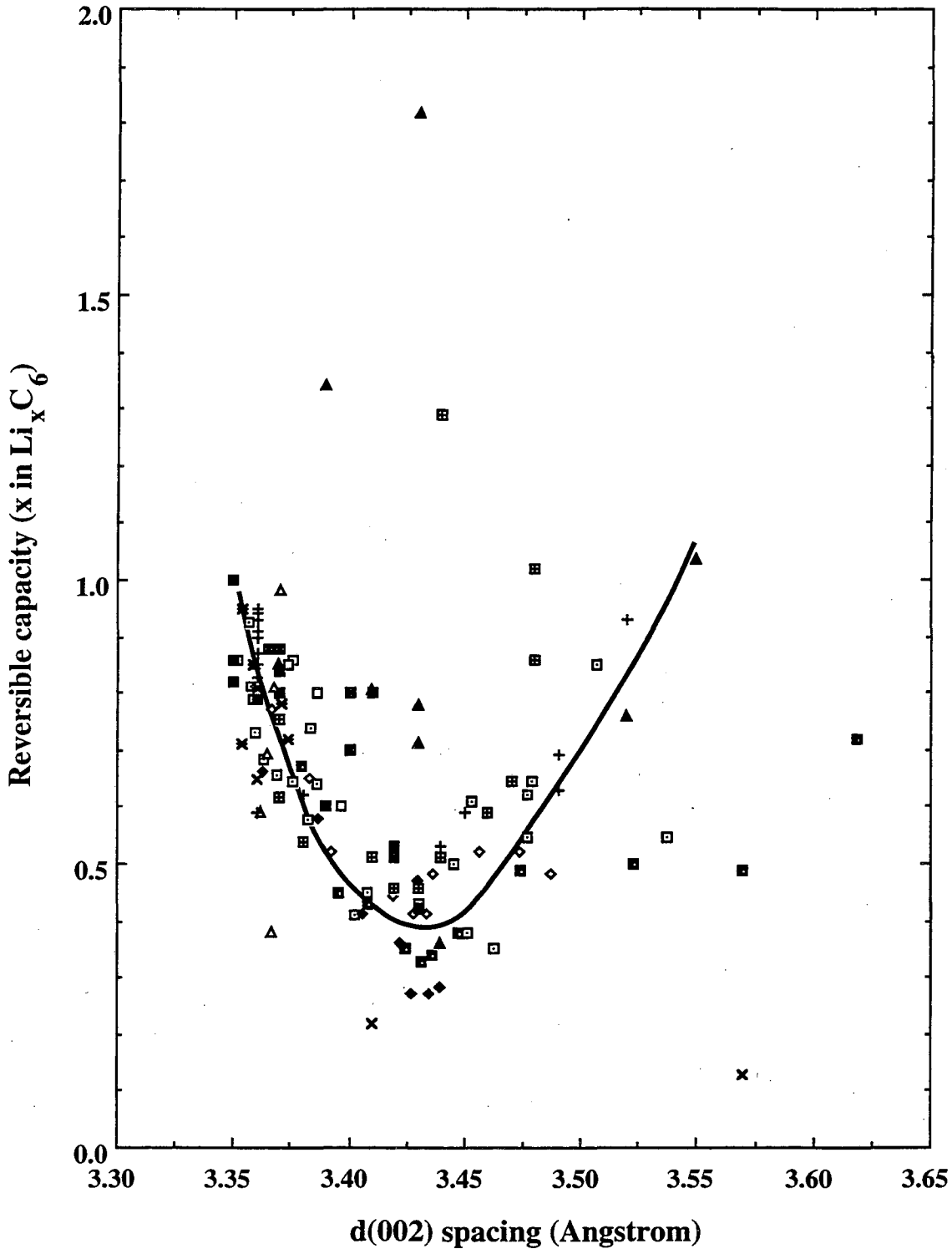

Figure 12. Experimental data for the Li storage capacity of carbonaceous materials and d(002) spacing of carbonaceous materials. Solid line represents the trend of the data points.

Table 1. Comparison of Lithium-Intercalated Carbon and Lithium Metal

Property	Li-C[a]	Li-graphite	Li Metal
Theoretical density (g/cm^3)	~1.0	2.25	0.53
Theoretical specific capacity (mAh/g)	>500	372	3862
Theoretical capacity density (mAh/cm^3)	>500	837	2047
Practical specific capacity (mAh/g)	>400	316[b]	772[c]
Practical capacity density (mAh/cm^3)	>400	506[b]	409[c]
Operating potential (V)	0.01-1.5	0.01-0.15	0-0.15

[a]based on amorphous carbon as the host for intercalation.
[b]85% active material.
[c]5-fold excess.

Table 2. Preparation of Lithiated Carbons by Non-Electrochemical Methods.

Carbon	Technique	Li-Intercalated Compound	Reference
Artificial graphite	Contact Li vapor and graphite at >500°C	1000°C: carbide, Li_2C_2 500°C: LiC_4 Li intercalation of graphite by cathodic polarization in molten KCl-LiCl at 400°C	Herold (1)
Madagscar and Ceylon graphite	Solution-phase reaction of graphite with Li naphthalenide in THF	Madagscar: $LiC_{17.5 \pm 1.5}$ Ceylon: $LiC_{43 \pm 3}$	Stein (61)
Ceylon graphite	React Li vapor with graphite	LiC_6, LiC_{18}, LiC_{28}, LiC_{36}, LiC_{72}	Bagouin (62)
Pyrolytic graphite	Immerse in liquid Li at 400°C for 2 h	LiC_6, bright metallic yellow color	Salzano (63)
Madagscar graphite	Solution-phase reaction of graphite and Li naphthalenide in DME	LiC_6 Total exclusion of DME without destruction of lamellar crystal is not possible	Minh-Duc (64)
Ceylon graphite	Compress Li + graphite mixture at 10-20 kbar, and heat at 200°C, 24 h React Li vapor with graphite at 400°C	1st, 2nd, 3rd or 4th stage LiC_6	Guerard (65, 66)
HOPG Polycrystalline spectroscopic graphite	Immerse in liquid Li at 350°C for 6-8 h	HOPG required 6-8 h and polycrystalline spectroscopic graphite required 4-5 h to form stage 1	Zanini (12)
Carbon fiber (CF)	Immerse in THF containing Li naphthalenide	Lamellar C_nLi obtained Electrical resistance is reduced by a factor of <7.5 compared with original CF Increase in HTT of CF and doping with B led to the formation of more highly satd. intercal. compds.	Fialkov (67)

Natural graphite Pyrolytic carbon, HT to 3200°C Needle coke HT to 1900°C	Immerse in THF or DME containing Li naphthalenide	LiC_6 obtained in DME with all carbons In THF, Li intercalation only in carbon with d(002) < 3.428 Å	Tanaike (67b)
HOPG (Union Carbide) Graphite (type PGCCL, Carbone Lorraine)	Immerse in Li-Na melt at ~150°C	1st, 2nd, 3rd stage	Billaud (36)
HOPG	Immerse in liquid Li metal or Li-Na alloy at 350°C, 8 h	Pure Li gives LiC_6 at equil. In 4% Li-Na, stage-2 formed	Basu (52)
HOPG	React Li vapor with graphite in evacuated vessel at ~400°C	No Li carbide found LiC_6 as well as higher stage compounds were produced	Pfluger (68)
HOPG	Immerse in Li-Na melt (composition NS) at 150°C, several hours	Stages 1-5 Two stage-2 compds. were reported: LiC_{12} in which Li atoms are ordered in a "hexal" type structure, and LiC_{18}, possessing a less-organized lacunar-type structure.	Billaud (69)
Graphite	Compress Li + graphite at <1000 MPa	<350 MPa, formed LiC_6 750 MPa, $C_{2.2+0.1}Li$	Semenenko (70)
Graphite	Compress Li + graphite at 2.0-8.0 GPa	$C_{2.0-2.5}Li$ limiting composition	Semenenko (71)
HOPG	Immerse in liquid Li metal at 200°C, 72 h	LiC_6	Pfluger(72)
Natural graphite	Stir graphite, Li metal and $Co(C_2H_4)(PMe_3)_3$ in pentane at 0°C, 24 h	LiC_6	Besenhard (73)
Graphite (Poco) Glassy carbon (GC)	Heat a mixture of graphite and GC with Li_2CO_3 at 1300 K for 24 h in vacuum	LiC_6	Jungblut (74)
LiC_6	React LiC_6 and Li at 1.5-2 GPa and 473-523 K or at 5-6 GPa and room temperature	LiC_2	Nalimova (75)

Graphite	Compress Li + graphite	Obtained compound with a Li/C ratio as high as 1/2. At ambient temperature and pressure, composition relaxes to close to Li_7C_{24}	Setton (76)
Graphite	Compress Li + graphite	Lower-stage compounds are formed as Li content increase	Oh (77)
Graphite	Compress Li + graphite	LiC_2-LiC_4	Guerard (78)

HOPG = highly oriented pyrolytic graphite, NS = not specified

Table 3. Examples of precursors, carbonaceous materials and companies involved in development of carbons for Li-ion batteries. Company names are underlined.

Carbon Black	Carbon Fiber	Coke	Graphite	Miscellaneous	Polymer-derived
acetylene black	petroleum	petroleum	artificial	HT high MW HC	glassy carbon
pyrolytic decomp. of benzene	HT polymer at 400-1200°C	coal	spectroscopic rod	CVD ammonia + chlorinated-benzene	acenaphthylene
Antralur	pitch	Kureha Chemical	foil, sheet	CVD benzene, 1000°C	poly(p-phenylene)
Black Pearls	vapor-grown	Asbury	natural, Brazil Madagascar	CVD propane	PAN
Vulcan XC-72	PAN	CONOCO	HOPG	decompose acetonitrile + pyridine	PFA
Ketjen black	phenol	Carbone Lorraine	pyrolytic	mesophase pitch-based microbeads	polyacenic semi-conductor
Sedena	coal tar	UNOCAL	nuclear	decompose acetonitrile or PAN+ BCl_3	PS
Super S	rayon	Repsol	Toshiba Ceramics Kish	Carbone Lorraine	PVA
Sterling R	Hyperion Catalysis	Nippon Steel Chemicals	Lonza (KS and SFG series)	Osaka Gas (MCMB) M1 - noncrystalline M2, M3 - graphitic	PTCDA
Mitsubishi	Petoca Ltd. (Melbion)	ANL Premium (coal)	Asbury	Nippon Sanso	PPCA
Cabot Corp.	Osaka Gas		Osaka Gas	Kawasaki Steel (MCMB)	PVDF, PVDC
	Nikkiso Co.		Mitsui Mining	sugar	Mitsubishi
	Nippon Steel		Superior Graphite	rf magnetron-sputtered carbon film	novolak resin
	Toray (T300B, T800HB, M46JB)		Toyo Carbon	coffee beans	polymethylacrylonitrile
	hydrocarbon gas		Sigri GmbH		Asahi Organic Chemicals (phenolic resin, furan resin)
	Great Lakes Carbon Corp. (Fortafil)		Chuetsu Graphite		phenol-formadehyde resin
	cellulose		Kansai Coke and Petrochemical (NG-7)		polyfluoranthene
			Nippon Kokuen		polypyrene
			Hitachi, metal-doped graphite		polypyrrole
			Sanyo, graphite-coke (4/1)		poly(hydrazocarbonyl-1,4-phenylenecarbonyl

PTCDA = 3,4,9,10-perylenetetra-3,4,9,10-carboxylic dianhydride, $C_{24}H_8O_8$.

Table 4. H/C atomic ratio for carbonized organic precursors.

Precursor	Carbonizing Temperature (°C)	H/C Atomic Ratio	Reference
Phenol-formaldehyde resin	600	0.27	104
	to	0.21	
	700	0.13	
Petroleum pitch (Kureha Co.)	550	0.41	105
	700	0.23	
	1000	0.04	
Petroleum pitch (Crowley Co.)	550	0.40	105
	700	0.21	
	1000	0.06	
PVC, polyvinyl chloride (Aldrich Chemical)	550	0.36	105, 106
	700	0.20	
	1000	0.05	
PVDF, polyvinylidene fluoride (Aldrich Chemical)	550	0.19	105
	700	0.07	
	1000	0.05	
PPS, polyphenylene sulfide (Aldrich Chemical)	700	0.29	105
	1000	0.04	
Novolac resin #DEN438 (Dow Chemical)	700	0.17	105
	1000	0.03	
Phenolic resin #11760 (Plenco)	700	0.19	107
	800	0.13	
	1000	0.05	
Phenolic resin #29217 (Oxychem)	700	0.22	106, 107
	800	0.11	
	1000	0.04	
Novolac resin #12116 (Plenco)	800	0.11	107
	1000	0.03	
Pyrene (Aldrich Chemical)	500	0.039	108
	700	0.04	
Sugar	700	0.18	109
	1000	0.05	

#DEN438, poly[phenyl glycidyl ether)-co-formaldehyde]

Table 5. Li storage capacity of carbonaceous materials in nonaqueous electrolytes.

Type/Source/ Property/Processing	Electrolyte	Li Storage Capacity (Rev. cap. unless otherwise noted)	Reference
Natural and Artifical Graphite			
HOPG	$LiClO_4$-PEO_8	340 mAh/g	Yazami (135)
Lonza KS15, 15.1 m^2/g Lonza KS6, 22.5 m^2/g	$LiAsF_6$-PC+EC	372 mAh/g at <0.4 V	Dahn (80)
Lonza	$LiAsF_6$ in PC+EC $LiASF_6$ in EC+EIG LNCS in EC+EIG LNCS in EC+DME	No difference in cycling with different electrolytes	Dahn (136)
Natural	EC or PC	370 mAh/g in EC; not intercalated in PC, gas evolution observed	Fujimoto (137)
Lonza KS15	$LiPF_6$ in EC and DEC.	350 mAh/g in EC-DEC In 100% DEC, no reversible cycling	Mao (138)
Lonza KS44	$LiAsF_6$ in MF, PC, EC, ethers and mixtures	335-372 mAh/g before degraded Worst performance in PC - no Li intercalation Addition of EC to MF improves electrode stability and cycle life	Aurbach (139)
Lonza , Asbury, Superior Graphite	LNCS in EC-DMC	372 mAh/g	Tran (140)
Synthetic Natural	$LiPF_6$ in EC-DMC	Cap. (mAh/g) 0.5 mA/cm^2 5 mA/cm^2 Synthetic 330 50 Natural 275 70 Higher de-intercalation rate with graphite than amorphous C	Zhang (141)
Natural, Kansai Coke and Chemical NG-7 Synthetic, Lonza KS-44	$LiClO_4$ in PC-DME	NG-7: 330-370 mAh/g KS-44: 360 mAh/g	Sawai (142)
Natural, Madagascar	$P(EO)_8LiClO_4$	280 mAh/g	Yazami (143, 144)
Natural, Nippon Kokuen, CSPE Chuetsu Graphite Works, BF5000	$LiClO_4$ in EC-DEC	CSPE: 265 mAh/g, coul. eff. 75.2% BF5000: 352 mAh/g, coul. eff. 76.3%	Iijima (145)
Lonza SFG15	$LiPF_6$ in EC-DEC	360 mAh/g, 97.9% coul. eff.	Takami (146)
Lonza KS15	$LiClO_4$ in chloro-EC and PC	359 mAh/g Irrev. cap 108 mAh/g (first cycle)	Shu (94)
Lonza R-Liba-D, air oxidized 600°C, 1.5 h Lonza R-Liba-S, air oxidized 550°C, 1.0 h	$LiPF_6$, $LiClO_4$, $LiAsF_6$ in EC, DEC, DMC, 1,3-dioxolane	Mild oxidation (burnoff) increased rev. cap. by 10-30% Irr. cap. decreased (for <6% burn-off) by about 10-20% Irr. cap. increased (for 30% burn-off) by about 70%	Peled (101)
Synthetic electrographite Natural, UF4 LeCarbone Lorraine	LNCS-solid polymer PEO	electrographite: 290 mAh/g after15 cycles UF4: 215 mAh/g after 8 cycles	Coowar (146)
F399 - mechanical grinding	$LiPF_6$ in EC-DMC	708 mAh/g, irrev. cap. 328 mAh/g	Disma (147)
Natural	$LiPF_6$ in DEC with PC, EC BC, SL, γ-BL	Solvent Cap. (mAh/g) EC/DEC 370 PC/DEC 0 BC/DEC 0 SL/DEC 0 γ-BL/DEC 0	Fujimoto (148)
Natural, UF4 LeCarbone Lorraine	$LiClO_4$ in EC	350 mAh/g at 7 mA/g	Naji (149)

Natural (China, Superior Graphite) Synthetic (Osaka Gas, Superior Graphite, Lonza)	$LiPF_6$ in EC-DMC	288-355 mAh/g	Shi (117)
Lonza SFG6, SFG15, SFG44	LNCS in EC-DMC	C/2 rate C/24 rate SFG6 298 mAh/g 372 mAh/g SFG44 93 mAh/g 372 mAh/g	Tran (150)
Petroleum and Coal-Based Cokes			
Conoco	$LiAsF_6$ in PC-EC	186 mAh/g at <1.1 V	Dahn (80)
Conoco	$LiClO_4$ in PC with dissolved crown ether	186 mAh/g	Tarascon (151)
Conoco	LNCS in PC+DME or EC+DME	186 mAh/g	Dahn (6)
Needle coke	$LiClO_4$-PC	179 mAh/g	Bittihn (152)
China	$LiClO_4$ in PC, DME, THF, 2Me-THF	>190 mAh/g coul eff. ~100% after 2nd cycle	Yang (153)
Calcined coal tar d(002) = 3.43 Å, L_c = 3.2 Å, L_a = 6.1 Å, SA = 4.2m^2/g.	$LiPF_6$/PC-DME	180 mAh/g Irrev. cap., 30 mAh/g	Yokoyama (154)
Petroleum- and pitch-based	EC or PC	180-240mAh/g	Fujimoto (137)
Petroleum- and pitch-based	$LiPF_6$ in EC	pitch (1200°C): 180 mAh/g petroleum (1400°): 250 mAh/g	Saito (155)
Coal coke, Le Carbone Lorraine	1M $LiBF_4$ in PC-EC-DME PEO-based polymer	370 mAh/g in liquid electrolyte 325 mAh/g in polymer electrolyte	Yazami (144, 156)
Repsol	$LiAsF_6$+LNCS in PC	253 mAh/g or 308 mAh/g with P-doping	Tran (140)
Coal coke	$P(EO)_8$-$LiClO_4$ 100°C	355 mAh/g	Yazami (157)
Petroleum coke	$LiPF_6$ in EC-DMC	250 mAh/g	Zhang (158)
Petroleum coke, HT 1000°C Kansai Coke and Chemical	$LiClO_4$ in PC-DME	350-450 mAh/g (0 - 2 V) 155 mAh/g (0 - 0.5 V)	Sawai (142)
Petroleum-based (C342) Pitch-based (P-coke) Needle (N-coke)	$LiClO_4$ in EC-DMC	Pet. coke has highest cap. (~200 mAh/g) during cycling and the lowest irrev. cap. loss during the first cycle	Chen (159)
Nippon Steel Chemical, Pitch-based coke A, random texture Pitch-based coke B, needle-like texture	$LiClO_4$ in EC-DEC	coke A : 300 mAh/g, coul. eff. 54.7% coke B : 317 mAh/g, coul. eff. 66.8%	Iijima (145)
Pitch-based	polymer electrolyte PEO-$LiClO_4$-PC-EC	102 mAh/g, coul. eff. >90%	Newnham (160)
Pitch-based HT 750° or 1000°C	$LiBF_4$ in PC	HT 750°C: 385 mAh/g HT 1000°C: 236 mAh/g	Mori (131)
HT 1900 or 2800°C	$LiClO_4$ in EC-DEC or PC-DMC	HTT (°C) Electrolyte Cap. (mAh/g) 2800 EC-DEC 14 2800 PC-DMC 8 1900 EC-DEC 147 1900 PC-DMC 236	Ma (167)
Pitch-based, HT 1200°C	$LiPF_6$ in EC-DEC	180 mAh/g	Doh (168)
Conoco	LNCS-solid polymer PEO	<100 mAh/g after 10 cycles	Coowar (214)
Pitch-based	$LiPF_6$ in DEC with PC, EC BC, SL, γ-BL	Solvent Cap. (mAh/g) EC/DEC 248 PC/DEC 247 BC/DEC 246 SL/DEC 245 γ-BL/DEC 244	Fujimoto (148)

Argonne National Laboratory Premium coal sample bank HT ~1000°C	$LiPF_6$ in EC-DEC	589-394 mAh/g	Zheng (120a)
Carbon Fiber			
Pitch-based, HT 2800°C	$LiClO_4$-PC $LiBF_4$-PC $LiAsF_6$-PC	230 mAh/g	Sato (169)
Pitch-based,10-μ m diameter	$LiClO_4$-PC+THF	220 mAh/g, ~100% coul. eff.	Morita (170)
Meso-pitch based, HT at 2800° or 1200°C	$LiClO_4$-PC+DME	37 mAh/g because diameter is too large	Imanishi (171)
Pitch-based	$LiClO_4$-PC, EC, DMSO γ-BL, or THF	>150 mAh/g, ~100% eff. with PC or EC Poor cycling in THF or BL No Li intercalation in DMSO	Iijima (172)
Vapor grown (VGCF)	$LiClO_4$ in PC+EC	185-208 mAh/g	Yamaura (173)
Pitch-based	$LiClO_4$ in EC, EC with 2Me-THF EC with 4Me-DOL	230 mAh/g	Suzuki (174)
Mesophase pitch	$LiPF_6$ or $LiAsF_6$ in PC	250-270 mAh/g	Takami (175)
Pitch-based (Shin-Nippon #01)	$LiClO_4$ in PC	>200 mAh/g	Matsuda (176)
Mesopitch (HT 2600° or 2800°C) Type A: radial texture with wedge, Type B: radial texture with fine zigzag layers	PC, THF, DEC, EC γ-BL, PC-THF	Type B, 130 mAh/g in PC+THF 160 mAh/g in PC 80 mAh/g in THF 35 mAh/g in DEC Type A, 220 mAh/g in γ-BL 220 mAh/g in EC Type A, Li cannot intercalate in PC and THF	Yamamoto (177)
Pitch-based with graphite structure	LiTf or $LiPF_6$ in EC or PC with DME, DEC, or DMC, LiTf	~200 mAh/g in LiTf/EC-based electrolyte Highest coul. eff. (98%) in LiTf/EC-DMC EC-based electrolyte with LiTf were better than those with $LiPF_6$	Matsuda (178)
Coal pitch-based, graphitized at 2800°C	$LiClO_4$ in PC	220 mAh/g was observed to 140th cycle	Uchida (179)
Pitch-based, graphitized	$LiClO_4$ in PC	220 mAh/g	Morita (180)
Pitch-based, 10-μ m diameter d(002) = 3.41 Å L_c =184 Å	LiTf and $LiPF_6$ in EC or PC mixed with 1,2-DME, DEC, or DMC	200 mAh/g in $LiCF_3SO_3$ in EC- based electrolytes Highest coul. eff. (98%) with LiTf in EC-DMC	Ishikawa (181)
Vapor grown; Nikkiso, 2GWH, HT 2800°C ~2 μm diam. ~10-μ m length 1A - whiskers graph. after chopping 2A - whiskers graph. before chopping	$LiClO_4$ in EC + DEC	Chopping fibers after graphization produced high rev. cap. (363 mAh/g) and high cycle life 1A whisker cap. 248 mAh/g 2A whisker cap. 363 mAh/g 2A whisker has higher defect structure, higher SA (10.7 versus 1.2 m^2/g) and larger L_c and L_a	Tatsumi (161)
PAN from Courtaulds Fibers, first oxidizing at 230-290°C in air, then pyrolyze in Ar at 900° or 1100°C	LiNCS in PC-DME LiTf, $LiBF_4$ or $LiAsF_6$ in PC	900° HT: 154 mAh/g in PC-DME 1100° HT: 333 mAh/g in PC-DME Max. cap. 472 mAh/g in PC obtained at oxid. T of 230°C and HT 1100°C Max rev. cap. depends on Li salt in PC: LiTf 465 mAh/g $LiBF_4$ 333 mAh/g $LiAsF_6$ 314 mAh/g	Levy (162)

Mesophase-based, Petoca Inc. (i) HT at 150-1000°C in vac. at several T; (ii) partial oxid. by HT at 700°C with covering of SAB; (iii) electrochem. red. and/or oxid. in nonaq. or aqueous electrolyte; (iv) silane couupling surface treatment	$LiClO_4$ in EC+PC or EC+DMC	Rev. cap. of carbon that is oxid. is lower (iii) gave higher cap. than as received sample (225 mAh/g) >300 mAh/g with (ii) No improved cap. with (iv)	Takamura (103)
Vapor grown, HT at 2800°C Nikkiso Co., Ltd.	$LiClO_4$ or $LiPF_6$ in EC-DEC	Rate (mAh/g) Capacity (mAh/g) 25 362 50 350 100 320 150 300 200 290	Tatsumi (163)
Nihon Carbon Co. GF-8	$LiClO_4$ in PC-DME	620 mAh/g (0 - 2 V) 150 mAh/g (0 - 0.5 V)	Sawai (142)
PAN-based, Toray T300 Isotropic pitch, Union Carbide UCC-2 and UCC-32 Pitch mesophase, Tonen FT 500 and FT 700	$LiBF_4$ in PC-EC-DME	Rev. cap. of mesophase-based electrodes increases with crystallinity FT700: 301 mAh/g FT500: 246 mAh/g UCC-2: 279 mAh/g UCC-32: 297 mAh/g T300:175 mAh/g	Yazami (143)
Graphite whiskers (2GWH-2A) Nikkiso, HT 2800°C ~2 μm diam., ~10 μm length	$LiClO_4$ in EC-DEC	363 mAh/g	Abe (164)
Graphitized Amoco, P 100-S	$LiClO_4$ in EC	268 mAh/g	Billaud (165)
Nippon Steel Chemical, pitch-based Toray Industries, PAN-based T300B, T800HB, M46JB	$LiClO_4$ in EC-DEC	pitch-based: 289 mAh/g, coul. eff. 96.3% PAN-based: 350mAh/g	Iijima (145)
Graphite whiskers (2GWH-2A) Nikkiso, HT 2800°C ~2 μm diam., ~10 μm length	$LiClO_4$, $LiBF_4$, $LiAsF_6$, $LiPF_6$, $LiCF_3SO_3$ in EC-DEC PEO-$LiClO_4$	Cap. decreaases $LiClO_4$ <$LiCF_3SO_3$ <$LiAsF_6$ <$LiPF_6$ <$LiBF_4$ $LiClO_4$-EC-DEC: 363 mAh/g PEO-$LiClO_4$: 330 mAh/g, 100% coul. eff. at 80°C	Zaghib (166)
Petoca Co. Ltd., HT 3000°C L_c = 350 Å d(002) = 3.366 Å (radial-like texture)	$LiPF_6$ in EC-DEC	305 mAh/g, 99.0% coul. eff.	Takami (146)
Pitch-based, 370-02, Nippon Steel Corp. d(002) = 3.41 Å L_c = 184 Å	$LiPF_6$, LiTf, $LiClO_4$ in PC, EC, DMC, DEC, DME	204 to 215 mAh/g Electrolyte composition as well as structure of electrode material greatly influenced charge/discharge profiles	Morita (182)
Mesophase pitch, treated with tri-Me silazane for modifying surface -OH group into tri-Me silyl group, HT 700°C	$LiClO_4$ in PC-EC or PC-DEC	>400 mAh/g	Takamura (183)
Mesophase pitch, Petoca carbonized at 650°C HT at 1000-3000°C	$LiClO_4$ in PC or EC-DMC	HT ~3000°C: >300 mAh/g, coul. eff. 92% HT <1000°C: >500 mAh/g, coul. eff. 70%	Tamaki (184)
Fortafil, Great Lakes Carbon Corp. (from PAN)	$LiClO_4$ in PC	298 mAh/g	Verbrugge (185)
Amoco pitch P100	$LiClO_4$ in EC	260 mAh/g at 7 mA/g	Naji (149)
Pyrolyzed Organic- or Polymer-Based			
HT PAN, 650-700°C 20-1100 m^2/g	$LiClO_4$ in PC	300 mAh/g	Sawtschenko (186)

PFA	$LiPF_6$ in PC+DEC or PC+DME	350 mAh/g	Sekai (187)
Deeply N-doped polyacenic semiconductors (PAS), HT phenol-formaldehyde resin at 600-700°C, d(002) > 4 Å	$LiPF_6$ in PC+DEC	H/C: 0.27, 0.21, 0.13 — Cap. (mAh/g): 530, 450, 300.	Yata (104, 188)
HT PFA <1000°C	$LiClO_4$ in PC+DME	>390 mAh/g, but poor cyclability	Imoto (189)
Pyrolyzed PFA + H_3PO_4 500-1300°C	$LiClO_4$ in PC+DME	450 mAh/g	Omaru (190)
HT poly(p-phenylene) 700°C H/C = 0.24	$LiPF_6$ in PC+DME	680 mAh/g	Sato (132)
Carbonize phenol-formaldehyde (PF) resin, PFA, PAN resins 650° - 750°C	$LiPF_6$ in EC-DEC	>450 mAh/g	Chu (191)
Thermal decomposition, 400°C BCl_3 + PAN ---> BC_3N BC_zN-Li_y	LiTf in EC-DMC	BC_zN, z = 2 (430 mAh/g); z = 4 (246 mAh/g); z = 10 (654 mAh/g)	Matsuda (192)
HT graphitizable acenaphthylene (AN) or coronene (CN), and non-graphitizable C from phenolphthalein (PH) at 800° and 1000°C	$LiClO_4$ in EC-DEC	Cap. (mAh/g): HTT (°C): 800, 1000, 2780; AN: 497, 264, 317; PH: 386, 282, 134	Tokumitsu (193)
PPP carbonized at 700-775°C	PAN-EC-LiX polymer electrolyte LiX = $LiClO_4$, $LiPF_6$, $LiAsF_6$, LNCS	Li salt — Cap. (mAh/g): $LiClO_4$ 710; $LiPF_6$ 487; $LiAsF_6$ 292; LNCS 412	Alamgir (194)
Pyrolyzed PAN, 600-1000°C density 0.35-0.5 g/cm^3 SA <50 m^2/g	LNCS or $LiAsF_6$ in PC	P-doped C (>2 at% P) 450 mAh/g which increased with increasing P content Pyrolysis at 600°C yielded 550 mAh/g, irrev. cap. 450 mAh/g Pyrolysis at 1000°C yielded 270 mAh/g, irrev. cap. 120 mAh/g	Tran (195)
Pet. pitch, Kureha Co. Pet. pitch, Crowley Tar Co. PVC, PVDF, PPS epoxy novolac resin HT 550° -1000°C	$LiPF_6$ in EC-DEC	Rev. cap. proportional to hydrogen content ~100 mAh/g, H/C ~0.03 940 mAh/g, H/C ~0.3	Zheng (105)
Polyacenic semiconductor (PAS)	$LiClO_4$ or $LiBF_4$ in PC	850 mAh/g C_2Li stage without Li-metal deposition	Yata (196, 197)
Pyrolysis of epoxy-silane composites DEN 438 epoxy novolac resin	$LiPF_6$ in EC-DEC	$C_{0.50}Si_{0.19}O_{0.31}$, 770 mAh/g, irrev. cap. 430 mAh/g Pure disordered carbon, 500 mAh/g, irrev. cap. 150 mAh/g	Xue (198)
3,4,9,10-perylenetetra-3,4,9,10-carboxylic dianhydride (PTCDA) HT 550° -1000°C	$LiPF_6$ in EC-PC	HT 550°C: 660 mAh/g, irrev. cap 380 mAh/g HT 1000°C: 295 mAh/g	Hara (199)
Epoxy resins, HT 1000°C	$LiPF_6$ in EC-DEC	570 mAh/g Chemisorbed oxygen (from oxidation treatment) appears to react with Li, and increases both irrev. and rev. cap.	Xue (200)
Resol and novolak resins HT 700° -1100°C	$LiPF_6$ in EC-DEC	Resol resin: HT 1000°C, ~550 mAh/g, little hysteresis, and good cycling performance	Zheng (107)
Pyrrole, fluoranthene and pyrene, HT 600°-3000°C	$LiClO_4$ in PC	fluoranthene HT 3000°C: 558 mAh/g pyrrole HT 3000°C: 5446 mAh/g	Hashizume (201)

poly-p-phenylene (PPP) HT 700° -3000°C	$LiClO_4$ in PC	680 mAh/g	Endo (202)
Condensed polynuclear aromatic (COPNA) synthesized from pyrene (Py) and a cross-linking agent, dimethyl-p-xylene glycol (DMPXG) HT 800°C	$LiClO_4$ in PC	Cap. increased as DMPXG/Py ratios increased >372 Ah/kg at >1.5 DMPXG/Py	Tokumitsu (122)
Phenolic resin (OXY), PVC HT 700°C	$LiPF_6$ in EC-DEC	Discharge cap. with large hysteresis were proportional to hydrogen content 30°C 70°C OXY: 500 mAh/g 700 mAh/g PVC : 600 mAh/g 800 mAh/g	Zheng (106)
Table sugar, HT 600° -1600°C	$LiPF_6$ in EC-DEC	~650 mAh/g, irrev. cap. ≤170 mAh/g	Xing (109)
Sugar, starch, nut shells, wood, lignin, phenolic resin Pyrolyzed 900° -1600°C	$LiPF_6$ in EC-DEC	Sugar: 260, 510, 650 mAh/g irrev. cap. 240, 140, 170 mAh/g oak: 193-536 mAh/g irrev. cap. 30-152 mAh/g nut shells: 383-508 mAh/g irrev. cap. 131-191 mAh/g resin: 560-330 mAh/g irrev. cap. 70-300 mAh/g	Xing (203)
Poly(phenyl glycidyl ether-co-formaldehyde) DEN438 Dow Chemical HT 900°, 1000° or 1100°C	$LiPF_6$ in EC-DEC	HT 900°C: 590 mAh/g HT 1000°C: 570-412 mAh/g HT 1100°C: 250 mAh/g	Liu (119)
Meso-Carbon Microbeads (MCMB)			
Osaka Gas, MCMB HT 1000° -2800°C	$LiClO_4$ in EC+DEC	Cap. (mAh/g) HTT (°C): 700 1200 2800 750 240 280	Mabuchi (121, 121b)
Mesophase pitch-based	$LiClO_4$ in PC+EC	Cap. (mAh/g) HTT (°C): 1000 2500 2800 173 208 240	Yamaura (173)
Mesophase pitch-based	$LiPF_6$ or $LiAsF_6$ in PC	250-270 mAh/g	Takami (175, 204)
HT 1000°, 2000°, 2800°C	$LiClO_4$ in PC, PC+DME, γ-BL, EC+2Me-THF, EC+DEE	2800°C, 140 mAh/g in PC+DME, 243 mAh/g in EC+DEE 1000°C, 180-250 mAh/g, not affected by electrolyte	Tatsumi (205)
Non-graphitized MCMB 6-10 Graphitized MCMB 6-28	$P(EO)_8$-$LiClO_4$ 100°C	MCMB 6-10: 410 mAh/g MCMB 6-28: 355 mAh/g	Yazami (144, 157)
Osaka Gas, MCMB HT 700° -1000°C	$LiClO_4$ in PC	HTT (°C) Cap. (mAh/g) Irrev. cap. (mAh/g) 700 750 440 800 485 352 900 382 274 1000 325 206	Fujimoto (206)
Osaka Gas, MCMB-6-28	$LiClO_4$ in EC-DEC	410 mAh/g, coul. eff. 87.3%	Iijima (145)
HT 1000° or 2800°C	$LiClO_4$ in EC-DEC or PC-DMC	HTT (°C) Electrolyte Cap.(mAh/g) 2800 EC-DEC 149 2800 PC-DMC 87 1000 EC-DEC 141 1000 PC-DMC 131	Ma (167)
MCMB 2510 - mechanical grinding	$LiPF_6$ in EC-DMC	708 mAh/g, irrev. cap. 328 mAh/g	Disma (147)
Carbon Black			

SAB, China	$LiClO_4$ in PC, DME, THF, 2Me-THF	>190 mAh/g coul eff. ~100% after 2nd cycle	Yang (153)
SAB	EC or PC	Li not intercalated in EC or PC and gas evolution observed	Fujimoto (137)
Cabot Sterling R	$LiPF_6$ + LNCS in PC	197 mAh/g or 346 mAh/g after HT 2800°C	Tran (140)
Shawinigan acetylene black	$P(EO)_8$-$LiClO_4$ 100°C	190 mAh/g	Yazami (144, 157)
Osaka Gas M-40	$LiClO_4$ in PC-DME	700-800 mAh/g (0 - 2 V) 45 mAh/g (0 - 0.5 V)	Sawai (142)
CVD/Vapor-Phase Doped-Carbon			
CVD of benzene at 1000°C	$LiClO_4$ in PC	350 mAh/g	Yoshimoto (207)
B-doped C, prepared by hot-wall CVD using BCl_3-benzene at 900°C B_zC_{1-z} (0<z<0.17)	LNCS in EC+PC	$Li_xB_zC_{1-z}$ (z ~0.1): 409 mAh/g $B_{0.17}C_{0.83}$: 437 mAh/g Irreversible capacity is not strongly affected by B doping	Way (208)
Vapor-phase reaction of acetonitrile and BCl_3 at 1000°C, then HT 1000°, 1500°, 2000°C; BC_2N	$LiClO_4$, $LiBF_4$, $LiAsF_6$ in PC, EC, DME	1500° (300 mAh/g) > 1000° > 2000° Higher cap. in EC-DME than PC-DME	Ishikawa (209)
N-doped carbons N_zC_{1-z} prepared at 900° -1000°C by CVD of C_2H_2 + NH_3 Hot-wall CVD using benzene and acetonitrile or pyridine	$LiAsF_6$ in DMC, PC, EC	Irrev. cap. loss increases with N content N/C (Wt%) Irrev. cap. (mAh/g) <0.1 17 2.9 72 8.37 183	Weydanz (210)
HT C_6H_6 + $SiCl_4$ at 950°C Si-doped C	$LiPF_6$ in PC-EC-DMC	at% Si cap. (mAh/g) 0 300 1.8 360 3.1 420 5.9 455 11 495	Wilson (211, 212)
HT saccharose, boric acid and urea at 1000°C	$LiClO_4$ or LiTf in EC-DME	$BC_{10}N$: 120 mAh/g $BC_{10}N$-$Li_{0.44}$: 100 mAh/g	Ishikawa (213)

cap. = capacity
coul. eff. = coulombic efficiency
HT = heat treat
irrev. = irreversible
LiTf = $LiCF_3SO_3$
LNCS, = $LiN(CF_3SO_2)_2$
PAN = polyacrylonitrile
PAS = polyacenic semiconductor
pet. = petroleum
PFA = polyfurfuryl alcohol
PPP = poly(p-phenylene)
PPS = polyphenylene sulfide
PS = polysulfone
PVA = polyvinyl alcohol
PVC = polyvinyl chloride
PVDF = polyvinylidenefluoride
rev. = reversible
SL = sulforan
VC = vinylidene chloride resin

Table 6. Influence of Electrolyte on the Reversible and Irreversible Capacity of Graphite and Coke.

Solvent ($LiPF_6$ salt)	Q_{rev} (mAh/g)		Q_{irrev} (mAh/g)		Q_{rev}/Q_t (%)	
	Coke	Graphite	Coke	Graphite	Coke	Graphite
EC/DEC (1:1)	248	370	56	34	82	92
PC/DEC (1:1)	247	0	58	gas evolution	81	0
BC/DEC (1:1)	246	0	58	gas evolution	81	0
SL/DEC (1:1)	245	0	56	153	81	0
γ-BL/DEC (1:1)	244	0	56	82	81	0

Source: Fujimoto et al. (148).

References

1. H. Boehm, R. Setton and E. Stumpp, Carbon, **24**, 241 (1986).

2. B. Scrosati, J. Electrochem. Soc., **139**, 2776 (1992).

3. M. Armand, in Materials for Advanced Batteries, D. Murphy, J. Broadhead and B. Steele, eds., Plenum Press, New York, p. 145 (1980).

4. T. Ohzuku, Y. Iwakoshi and K. Sawai, J. Electrochem. Soc., **140**, 2490 (1993).

5. K. Brandt, R. Herr and Hoge, DECHEMA Monogr., **128** (Elektrochemische Energiegewinnung), 279 (1993).

6. J. Dahn, U. von Sacken, M. Juzkow and H. al-Janaby, J. Electrochem. Soc., **138**, 2207 (1991).

7. S. Megahed and B. Scrosati, J. Power Sources, **51**, 79 (1994).

8. J. Besenhard and M. Winter, in Ladungsspeicherung Doppleschicht, Tagungsband, W. Schmickler, ed., Ulmer Elektrochem. Tage, 2nd, 1994, Universitaetsverlag, Ulm. Germany, p. 47 (1995).

9. J. Tarascon and D. Guyomard, Electrochim. Acta, **38**, 1221 (1993); D. Guyomard and J. Tarascon, Solid State Ionics, **69**, 222 (1994).

10. S. Hossain, in Handbook of Batteries, Second Edition, D. Linden, ed., McGraw-Hill, Inc., New York, p. 36.1 (1995).

11. A. Herold, Bull. Soc. Chim. Fr., **187**, 999 (1955).

12. M. Zanini, S. Basu and J. Fischer, Carbon, **16**, 211 (1978).

13. M. Zanini, L-Y. Ching and J. Fischer, Phys. Rev. B, **18**, 2020 (1978).

14. C. Ayache, E. Bonjour, R. Lagnier and J. Fischer, Physica, **99B**, 547 (1980).

15. D. DiVincenzo, C. Fuerst and J. Fischer, Phys. Rev. B, **29**, 1115 (1984).

16. G. Doll, P. Eklund and J. Fischer, Phys. Rev. B, **36**, 4940 (1987).

17. W. Eberhardt, I. McGovern, E. Plummer and J. Fischer, Phys. Rev. Lett., **44**, 200 (1980).

18. P. Eklund, G. Dresselhaus, M. Dresselhaus and J. Fischer, Phys. Rev. B, **21**, 4795 (1980).

19. T. Fauster, F. Himpsel, J. Fischer and E. Plummer, Phys. Rev. Lett., **51**, 430 (1983).

20. J. Fischer, Physica, **99B**, 383 (1980).

21.J. Fischer, C. Fuerst and K. Woo, Synth. Met., **7**, 1 (1983).

22.J. Fischer and H. Kim, Phys. Rev. B, **35**, 3295 (1985).

23. J. Fischer and H. Kim, Synth. Met., **23**, 121 (1988).

24. J. Fischer and H. Kim, Synth. Met., **12**, 137 (1985).

25. L. Grunes, I. Gates, J. Ritsko, E. Mele, D. DiVincenzo, M. Preil and J. Fischer, Phys. Rev. B, **28**, 6681 (1983).

26. S. Ikehata, J. Milliken, A. Heeger and J. Fischer, Phys. Rev. B, **25**, 25 (1982).

27. N. Kambe, M. Dresselhaus, G. Dresselhaus, S. Basu, A. McGhie and J. Fischer, Mat. Sci. Eng., **41**, 1 (1979).

28. H. Kim, A. Magerl, J. Soubeyroux and J. Fischer, Phys. Rev. B, **39**, 4670 (1989).

29. I. McGovern, W. Eberhardt, E. Plummer and J. Fischer, Physica, **99B**, 415 (1980).

30. J. Rossat-Mignod, D. Fruchart, M. Moran, J. Milliken and J. Fischer, Synth. Met., **2**, 143 (1980).

31. J. Rossat-Mignod, A. Wiedenmann, K. Woo, J. Milliken and J. Fischer, Solid State Comm., **44**, 1339 (1982).

32. A. Schirmer, J. Fischer, P. Heitjans, H. Kim, A. Magerl, D. Vaknin and H. Zabel, Mol. Cryst. Liq. Cryst., **244** (Section A), 299 (1994).

33. A. Schirmer, P. Heitjans, W. Faber and J. Fischer, Synth. Met., **34**, 589 (1990).

34. K. Woo, W. Kamitakahara, D. DiVincenzo, D. Robinson, H. Mertwoy, J. Milliken and J. Fischer, Phys. Rev. Lett., **50**, 182 (1983).

35. K. Woo, H. Mertwoy, J. Fischer, W. Kamitakahara and D. Robinson, Phys. Rev. B, **27**, 7831 (1983).

36. D. Billaud, E. McRae and A. Herold, Mat. Res. Bull., **14**, 857 (1979).

37. P. Delhaes, J. Amiell, K. Ohhashi, J. Mareche, D. Guerard and A. Herold, Synth. Met., **8**, 269 (1983).

38. E. McRae, D. Billaud, J. Mareche and A. Herold, Physica B+C, **99**, 498 (1980).

39. A. Dey and B. Sullivan, J. Electrochem. Soc., **117**, 222 (1970).

40. J. Dunning, W. Tiedemann, L. Hsueh and D. Bennion, J. Electrochem. Soc., **118**, 1886 (1971).

41. J. Besenhard and H. Fritz, J. Electroanal. Chem., **53**, 329 (1974).

42. J. Besenhard, Carbon, **14**, 111 (1976).

43. G. Eichinger, J. Electroanal. Chem., **74**, 183 (1976).

44. M. Armand and P. Touzain, Mat. Sci. Eng., **31**, 319 (1977).

45. P. Pfluger, H. Kunzi and H. Guntherodt, Appl. Phys. Lett., **35**, 771 (1979).

46. S. Basu, "Rechargeable Batteries," Bell Laboratories, USP 4,304,825, December 8, 1981.

47. S. Basu, "Ambient Temperature Rechargeable Batteries," Bell Laboratories, USP 4,423,125, December 27, 1983.

48. K. Kinoshita, *Carbon Electrochemical and Physicochemical Properties*, Wiley and Sons, New York (1988).

49. M. Studebaker and C. Snow, J. Phys. Chem., **59**, 973 (1955).

50. P. Delhaes and F. Carmona, in Chemistry and Physics of Carbon, P. Walker and P. Thrower, eds., Dekker, New York, p. 89 (1981).

51. D. Guerard and A. Herold, Carbon, **13**, 337 (1975).

52. S. Basu, C. Zeller, P. Flanders, C. Fuerst, W. Johnson and J. Fischer, Mat. Sci. Eng., **38**, 275 (1979).

53. N. Holzwarth, L. Girifalco and S. Rabii, Phys. Rev. B, **18**, 5206 (1978).

54. V. Nalimova and K. Semenenko, Carbon, **32**, 1019 (1994).

55. J. Conard, V. Nalimova and D. Guerard, Mol. Cryst. Liq. Cryst., **245** (Section A), 25 (1994).

56. L. Seger, L-Q. Wen and J. Schlenoff, J. Electrochem. Soc., **138**, L81 (1991).

57. R. Compton, R. Spackman, D. Riley, R. Wellington, J. Eklund, A. Fischer, M. Green, R. Doothwaite, A. Stephens and J. Turner, J. Electroanal. Chem., **344**, 235 (1993).

58. E. Dalchiele, J. Rosolen and F. Decker, Applied Physics A - Mater. Sci. Processing, **63**, 487 (1996).

59. R. Yazami and A. Cherigui, Extended Abstracts, Seventh International Meeting on Lithium Batteries, May 15-20, 1994, Boston, MA, p. 255 (1994).

60. R. Yazami and A. Cherigui, Mol. Cryst. Liq. Cryst., **244** (Section A), 209 (1994).

61. C. Stein, L. Bonnetain and J. Gole, Bull. Soc. Chim. Fr., 3166 (1966).

62. M. Bagouin, D. Guerard and A. Herold, C.R. Acad. Sci., Paris, **262C**, 557 (1966).

63. F. Salzano, S. Aronson and A. Ingraham, J. Amer. Ceram. Soc., **51**, 465 (1968).

64. C. Minh-Duc, C. Mai, R. Riviere and J. Gole, J. Chim. Phys. **69**, 69 (1972).

65. D. Guerard and A. Herold, C.R. Acad. Sci., Paris, **275C**, 571 (1972).

66. D. Guerard and A. Herold, Carbon, **13**, 337 (1975).

67. A. Fialkov, T. Zhuikova, T. Kaz'mina, N. Savost'yanova, Y. Novikov, Izv. Akad. Nauk SSSR, Neorg. Mater., **14**, 1844 (1978).

67b. O. Tanaike and M. Inagaki, Carbon, **35**, 831 (1997).

68. P. Pfluger, V. Geiser, S. Stolz and H. Guntherodt, Synth. Met., **3**, 27 (1981).

69. D. Billaud, E. McRae, J. Mareche and A. Herold, Synth. Met., **3**, 21 (1981).

70. K. Semenenko, V. Avdeev and V. Mordkovich, Russ. J. Inorg. Chem., **29**, 1277 (1984); V. Avdeev, V. Mordkovich and K. Semenenko, Vestn. Mosk. Univ., Ser. 2; Khim., **23**, 501 (1982).

71. K. Semenenko, V. Avdeev and V. Mordkovich, Russ. J. Phys. Chem., **271**, 273 (1984); V. Mordkovich, VINITI, **363**, 7085 (1983).

72. P. Pfluger, K. Muller, W. Berlinger, V. Geiserand and H. Guntherodt, Synth. Met., **8**, 15 (1983).

73. J. Besenhard, H. Witty and H. Klein, Carbon, **22**, 97 (1983); see also, H. Klein, M. Dreisbach, M. Gass and G. Cordier, Mater. Sci. Forum, 91-93 (Intercalation Compd., Pt. 1), **78-3** (Inorganic Chemicals and Reactions), 35 (1992).

74. B. Jungblut, E. Hoinkis, U. Dobler and H. Meyerheim, Ber. Bunsenges. Phys. Chem., **93**, 1317 (1989).

75. V. Nalimova, V. Avdeev, I. Udod and K. Semenenko, Zh. Obshch. Khim., **60**, 868 (1990).

76. R. Setton and J. Conard, Mol. Cryst. Liq. Cryst., **244** (Section A), 307 (1994).

77. W. Oh, Y. Kim and Y. Ko, Anal. Sci. Technol., **7**, 315 (1994).

78. D. Guerard and V. Nalimova, Mol. Cryst. Liq. Cryst., **244** (Section A), 263 (1994); J. Conard, V. Nalimova and Guerard, Mol. Cryst. Liq. Cryst., **244** (Section A), A25 (1994).

79. R. Clarke and C. Uher, Adv. Phys., **33**, 469 (1984).

80. R. Fong, U. von Sacken and J. Dahn, J. Electrochem. Soc., **137**, 2009 (1990).

81. M. Terasaki, H. Yoshida, T. Fukunaga, H. Tukamoto, M. Mizutani and M. Yamachi, GS News Tech. Rept., **53**, 23 (1994).

81b. A. Naji, J. Ghanbaja, P. Willmann and D. Billaud, Carbon, **35**, 845 (1997).

82. K. Takei, K. Kumai, Y. Kobayashi, H. Miyashiro, T. Iwahori, T. Uwai and H. Ue, J. Power Sources, **54**, 171 (1995).

83. E. Peled, in Lithium Batteries, J.P. Gabano, ed., Academic Press, London, England, p. 43 (1983).

84. D. Aurbach, Y. Ein-Eli, B. Markovsky, A. Zaban, S. Luski, Y. Carmeli and H. Yamin, J. Electrochem. Soc., **142**, 2882 (1995).

85. D. Aurbach, B. Markovsky, A. Shechter and Y. Ein-Eli,, J. Electrochem. Soc., **143**, 3809 (1996).

86. Y. Ein-Eli, S. Thomas, R. Chadha, T. Blakley and V. Koch, J. Electrochem. Soc., **144**, 823 (1997).

87. Z. Shu, R. McMillan and J. Murray, J. Electrochem. Soc., **140**, 922 (1993).

88. Z. Shu, R. McMillan and J. Murray, in Proceedings of the Symposium on New Sealed Rechargeable Batteries and Supercapacitors, B. Barnett, E. Dowgiallo, G. Halpert, Y. Matsuda and Z. Takehara, eds., The Electrochemical Society Inc., Pennington, NJ, p. 228 (1993) .

89. J. Besenhard, M. Wagner, M. Winter, A. Jannakoudakis, P. Jannakoudakis and E. Theodoridou, J. Power Sources, **44**, 412 (1993).

90. J. Besenhard, M. Winter, J. Yang and W. Biberacher, J. Power Sources, **54**, 228 (1995).

91. Z. Shu, R. McMillan and J. Murray, J. Electrochem. Soc., **140**, L101 (1993).

92. Y. Roh, K. Tada, T. Kawai, H. Araki, K. Yoshino, M. Takase and T. Suzuki, Japanese J. Appl. Phys. Part 2 - Letters, **34**, L61 (1995).

93. Y. Roh, T. Kawai, H. Araki, K. Yoshino, M. Takase and T. Suzuki, Synth. Met., **69**, 601 (1995).

94. Z. Shu, R. McMillan, J. Murray and I. Davidson, J. Electrochem. Soc., **142**, L161 (1995).

95. Z. Shu, R. McMillan, J. Murray and I. Davidson, J. Electrochem. Soc., **143**, 2230 (1996).

96. T. Uchida, Y. Morikawa and M. Wakihara, Extended Abstracts, 183rd Meeting of The Electrochemical Society, Inc., May 16-21, 1993, Honolulu, HI, Abstract #73, p. 109.

97. J. Yamaki, Hyomen Gijutsu, **45**, 21 (1994).

98. O. Yamamoto, Y. Takeda and N. Imanishi, in Proceedings of the Symposium on New Sealed Rechargeable Batteries and Supercapacitors, B. Barnett, E. Dowgiallo, G. Halpert, Y. Matsuda and Z. Takehara, eds., The Electrochemical Society Inc., Pennington, NJ, p. 302 (1993).

99. E. Peled, D. Bar Tow, A. Melman, E. Gerenrot, Y. Lavi and Y. Rosenberg, in Proceedings of the Symposium on Lithium Batteries, N. Doddapaneni and A. Landgrebe, eds., The Electrochemical Society Inc., Pennington, NJ. p. 177 (1994).

100. E. Peled, D. Golodnitsky, G. Ardel, C. Manachem, D. Bar Tow and V. Eshkenazy, in Proceedings of the Symposium on Materials for Electrochemical Energy Storage and Conversion-Batteries, Capacitors and Fuel Cells, Mater. Res. Soc. Symp. Proc. 393, D. Doughty, B. Vjas, T. Takamura and J. Huff, eds., MRS, Pittsburgh, PA, p. 209 (1995).

101. E. Peled, C. Menachem, D. Bartow and A. Melman, J. Electrochem. Soc., **143**, L4 (1996).

102. T. Takamura, N. Kikuchi, J. Ebana, M. Nagashima and Y. Ikezawa, in Proceedings of the Symposium on Rechargeable Lithium and Lithium-Ion Batteries, S. Megahed, B. Barnett and L. Xie, eds., The Electrochemical Society Inc., Pennington, NJ, p. 228 (1994).

103. T. Takamura, N. Kikuchi, and Y. Ikezawa, in Proceedings of the Symposium on Rechargeable Lithium and Lithium-Ion Batteries, S. Megahed, B. Barnett, and L. Xie, eds., The Electrochemical Society Inc., Pennington, NJ, p. 213 (1994).

103b. J. Brooks and G. Taylor, Carbon, **3**, 185 (1961).

103c. J. Brooks and G. Taylor, in Chemistry and Physics of Carbon, Vol. 4, P. Walker, ed., Marcel Dekker, New York, p. 248 (1968).

103d. H. Honda, Carbon, **28**, 139 (1988).

103e. M. Kodama, T. Fujiura, E. Ikawa, K. Esumi, K. Meguro and H. Honda, Carbon, **30**, 43 (1990).

103f. O. Yamamoto, Y. Takeda, R. Kanno, K. Nakanishi and T. Ichikawa, in Proceedings of the Symposium on Primary and Secondary Ambient Temperature Lithium Batteries, J. Gabano, Z. Takehara and P. Bro, eds., The Electrochemical Society Inc., Pennington, NJ, p. 754 (1988).

104. S. Yata, H. Kinoshita, M. Komori, N. Ando, K. Tanaka and T. Yamabe, in Proceedings of the Symposium on New Sealed Rechargeable Batteries and Supercapacitors, B. Barnett, E. Dowgiallo, G. Halpert, Y. Matsuda and Z. Takehara, eds., The Electrochemical Society Inc., Pennington, NJ, p. 502 (1993).

105. T. Zheng, Y. Liu, E. Fuller, S. Tseng, U. von Sacken and J. Dahn, J. Electrochem. Soc., **142**, 2581 (1995).

106 T. Zheng, W. McKinnon and J. Dahn, J. Electrochem. Soc., **143**, 2137 (1996).

107. T. Zheng, Q. Zhong and J. Dahn, J. Electrochem. Soc., **142**, L211 (1995).

108. G. Sandi, R. Winans and K. Carrado, J. Electrochem. Soc., **143**, L95 (1996).

109. W. Xing, J. Xue and J. Dahn, J. Electrochem. Soc., **143**, 3046 (1996).

110. J. Dahn, A. Sleigh, H. Shi, J. Reimers, Q. Zhong and B. Way, Electrochim. Acta, **38**, 1179 (1993).

111. J. Shi, J. Reimers and J. Dahn, J. Appl Crystal., **26**, 827 (1993).

112. R. Franklin, Acta Cryst., **4**, 253 (1951).

113. R. Franklin, Acta Cryst., **3**, 107 (1950).

114. B. Warren, J. Chem. Phys., **2**, 551 (1934).

115. B. Warren, Phys. Rev., **59**, 693 (1941).

116. J. Biscoe and B. Warren, J. Appl. Phys., **13**, 364 (1942).

117. H. Shi, J. Barker, M. Saidi and R. Koksbang, J. Electrochem. Soc., **143**, 3466 (1996).

117b. S. Flandrois, A. Fevrier, J. Biensan and B. Simon, "Carbon Anode for a Lithium Rechargeable Electrochemical Cell and a Process for its Production," SAFT, U.S. Patent 5,554,462 (Sept. 10, 1996).

118. W. Xing, J. Xue, T. Zheng, A. Gibaud and J. Dahn, J. Electrochem. Soc., **143**, 3482 (1996).

119. Y. Liu, J. Xue, T. Zheng and J. Dahn, Carbon, **34**, 193 (1996).

120a. T. Zheng, W. Xing and J. Dahn, Carbon, **34**, 1501 (1996).

120b. P. Zhou, P. Papanek, R. Lee, J. Fscher and W. Kamitakakara, J. Electrochem. Soc., **144**, 1744 (1997).

120c. J. Dahn, W. Xing and Y. Gao, Carbon, **35**, 825 (1997).

121. A. Mabuchi, K. Tokumitsu, H. Fujimoto and T. Kasuh, J. Electrochem. Soc., **142**, 1041 (1995).

121b. A. Mabuchi, H. Fujimoto, K. Tokumitsu and T. Kasuh, T., J. Electrochem. Soc., **142**, 3049 (1995).

122. K. Tokumitsu, A. Mabuchi, H. Fujimoto and T. Kasuh, J. Electrochem. Soc., **143**, 2235 (1996).

123. A. Mabuchi, H. Fujimoto, N. Yamanishi, T. Kasuh, R. Fujii, K. Tassumi, S. Higuchi and T. Maeda, Extended Abstracts, 183rd Meeting of The Electrochemical Society, Inc., May 16-21, 1993, Honolulu, HI, Abstract #64, p. 95.

124. H. Fujimoto, A. Mabuchi, K. Tokumitsu and T. Kasuh, Carbon, **32**, 193 (1994).

125. H. Fujimoto, A Mabuchi, K. Tokumitsu and T. Kasuh, Carbon, **32**, 1249 (1994).

126. J. Dahn, T. Zheng, Y. Liu and J. Xue, Science, **270**, 590 (1995).

127. P. Papanek, M. Radosavljevic and J. Fischer, Chem. Mater., **8**, 1519 (1996).

128. M. Nakadaira, R. Saito, T. Kimura, G. Dresselhaus and M. Dresselhaus, J. Mater. Res., **12**, 1367 (1997).

129. Y. Matsumura, S. Wang and J. Mondori, Carbon, **33**, 1457 (1995).

130. S. Wang, Y. Matsumura and T. Maeda, Synth. Met., **71**, 1759 (1995).

131. Y. Mori, T. Iriyama, T. Hashimoto, S. Yamazaki, F. Kawakami and H. Shiroki, J. Power Sources, **56**, 205 (1995).

132. K. Sato, M. Noguchi, A. Demachi, N. Oki and M. Endo, Science, **264**, 556 (1994).

133. K. Sato, M. Noguchi, A. Demachi, N. Oki, M. Endo and Y. Sasabe, in Proceedings of International Workshop on Advanced Batteries (Lithium Batteries), February 22-24, 1995, Osaka, Japan, Science and Technology Agency of Japan, Tokyo, Japan, p. 219 (1995).

134. S. Wang, Y. Shang, L. Yang and Q. Liu, Solid State Ionics, **86-88**, 919 (1996).

135. R. Yazami and P. Touzain, J. Power Sources, **9**, 365 (1983).

136. J. Dahn, R. Fong and M. Spoon, Phys. Rev. B, **42**, 6424 (1990).

137. M. Fujimoto, K. Ueno, T. Nohma, M. Takahashi, K. Nishio, and T. Saito, Extended Abstracts, 183rd Meeting of The Electrochemical Society, Inc., May 16-21, 1993, Honolulu, HI, Abstract #72, p. 108.

138. H. Mao, P. Juric and U. von Sacken, Extended Abstracts, 184th Meeting of The Electrochemical Society, Inc., October 10-25, 1993, New Orleans, LA, Abstract #38, p. 64.

139. D. Aurbach, Y. Eineli, O. Chusid, Y. Carmeli, M. Babai and H. Yamin, J. Electrochem. Soc., **141**, 603 (1994).

140. T. Tran, J. Feikert, S. Mayer, X. Song and K. Kinoshita, in Proceedings of the Symposium on Rechargeable Lithium and Lithium-Ion Batteries, S. Megahed, B. Barnett and L. Xie, eds., The Electrochemical Society Inc., Pennington, NJ, p. 110 (1994); T. Tran, J. Feikert, X. Song and K. Kinoshita, J. Electrochem. Soc., **142**, 3297 (1995).

141. Z. Zhang, in Proceedings of the Symposium on Rechargeable Lithium and Lithium-Ion Batteries, S. Megahed, B. Barnett and L. Xie, eds., The Electrochemical Society Inc., Pennington, NJ, p. 165 (1994).

142. K. Sawai, Y. Iwakoshi and T. Ohzuku, Solid State Ionics, **69**, 273 (1994).

143. R. Yazami, K. Zaghib and M. Deschamps, J. Power Sources, **52**, 55 (1994).

144. R. Yazami and M. Deschamps, J. Power Sources, **54**, p. 411, 1995; in Proceedings of the Symposium on Rechargeable Lithium and Lithium-Ion Batteries, S. Megahed, B. Barnett and L. Xie, eds., The Electrochemical Society Inc., Pennington, NJ, p. 183 (1994).

145. T. Iijima, K. Suzuki and Y. Matsuda, Synthetic Met., **73**, 9 (1995).

146. N. Takami, A. Satoh, M. Hara and T. Ohsaki, J. Electrochem. Soc., **142**, 2564 (1995).

147. F. Disma, L. Aymard, L. Dupont and J. Tarascon, J. Electrochem. Soc., **143**, 3959 (1996).

148. M. Fujimoto, Y. Kida, T. Nohma, M. Takahashi, K. Nishio and T. Saito, J. Power Sources, **63**, 127 (1996).

149. A. Naji, J. Ghanbaja, B. Humbert, P. Willmann and D. Billaud, J. Power Sources, **63**, 33 (996).

150. T. Tran, J. Feikert, R. Pekala and K. Kinoshita, J. Appl. Electrochem., **26**, 1161 (1996).

151. J. Tarascon and D. Guyomard, J. Electrochem. Soc., **138**, 2864 (1991).

152. R. Bittihn, R. Herr, and D. Hoge, presented at the 6th International Meeting on Lithium Batteries, Munster, Germany, May 10-15, 1992.

153. H. Yang, X. Ai, and S. Li, presented at the 6th International Meeting on Lithium Batteries, Munster, Germany, May 10-15, 1992.

154. K. Yokoyama and M. Nakagawa, Extended Abstracts, 183rd Meeting of The Electrochemical Society, Inc., May 16-21, 1993, Honolulu, HI, Abstract #70, p. 104.

155. T. Saito, T. Nohama, M. Takahashi, M. Fujimoto and K. Nishio, in Proceedings of the Symposium on New Sealed Rechargeable Batteries and Supercapacitors, B. Barnett, E. Dowgiallo, G. Halpert, Y. Matsuda, and Z. Takehara, eds., The Electrochemical Society Inc., Pennington, NJ, p. 355 (1993).

156. R. Yazami, K. Zaghib, and M. Deschamps, Mol. Cryst. Liq. Cryst., **245** (Section A), 165 (1994).

157. R. Yazami and M. Deschamps, Extended Abstracts, 186th Meeting of The Electrochemical Society, Inc., October 9-14, 1994, Miami, FL., Abstract #94, p. 148.

158. Z. Zhang, Extended Abstracts, 186th Meeting of The Electrochemical Society, Inc., October 9-14, 1994, Miami, FL., Abstract #93, p. 146.

159. J. Chen, C. Yao, C. Cheng, W. Hurng and T. Kao, J. Power Sources, **54**, 494 (1995).

160. C. Newnham, S. Rinne and N. Scholey, J. Power Sources, **54**, 516, (1995).

161. K. Tatsumi, K. Zaghib, H. Abe, S. Higuchi, T. Ohsaki and Y. Sawada, J. Power Sources, **54**, 425 (1995).

162. S. Levy, S. Klassen and R. Lagasse, in Proceedings of the Symposium on Rechargeable Lithium and Lithium-Ion Batteries, S. Megahed, B. Barnett and L. Xie, eds., The Electrochemical Society Inc., Pennington, NJ, p. 207 (1994).

163. K. Tatsumi, K. Zaghib, H. Abe, T. Ohsaki, S. Higuchi and Y. Sawada, Extended Abstracts, 186th Meeting of The Electrochemical Society, Inc., October 9-14, 1994, Miami, FL., Abstract #142, p. 223.

164. H. Abe, K. Zaghib, K. Tatsumi and S. Higuchi, J. Power Sources, **54**, 236 (1995).

165. D. Billaud, F. Henry and P. Willmann, J. Power Sources, **54**, 383 (1995).

166. K. Zaghib, K. Tatsumi, H. Abe, T. Ohsaki, Y. Sawada and S. Higuchi, J. Power Sources, **54**, 435 (1995); in Proceedings of the Symposium on Rechargeable Lithium and Lithium-Ion Batteries, S. Megahed, B. Barnett and L. Xie, eds., The Electrochemical Society Inc., Pennington, NJ, p. 121 (1994).

167. S. Ma, J. Li, B. Xia and F. Wang, Chin. Chem. Lett., **7**, 389 (1996).

168. C. Doh, S. Moon, W. Kim and M.Yun, Bull. Korean Chem. Soc., **17**, 861 (1996).

169. M. Sato, T. Iijima, K. Suzuki, and K. Fujimoto, in Proceedings of the Symposium on Primary and Secondary Lithium Batteries, K. Abraham and M. Salomon, eds., The Electrochemical Society, Inc., Pennington, NJ, p. 407 (1991).

170. M. Morita, N. Nishimura, H. Tsutsumi, and Y. Matsuda, Chem. Express, **6**, 619 (1991).

171. N. Imanishi, S. Ohashi, Y. Takeda, O. Yamamoto, and M. Inagaki, in Proceedings of the Symposium on High Power, Ambient Temperature Lithium Batteries, W. Clark and G. Halpert, eds., The Electrochemical Society, Inc., Pennington, NJ, p. 80 (1992).

172. T. Iijima, K. Suzuki, M. Tokumitsu, and M. Sato, Extended Abstracts, 180th Meeting of The Electrochemical Society, Inc., October 13-17 1991, Phoenix, AZ, Abstract #32, p. 58.

173. J. Yamaura, Y. Ozaki, A. Morita, and A. Ohta, presented at the 6th International Meeting on Lithium Batteries, Munster, Germany, May 10-15, 1992.

174. K. Suzuki, T. Iijima, and M. Sato, presented at the 6th International Meeting on Lithium Batteries, Munster, Germany, May 10-15, 1992.

175. N. Takami, A. Sato and T. Ohsaki, in Proceedings of the Symposium on Lithium Batteries, S. Surampudi and V. Koch, eds., The Electrochemical Society Inc., Pennington, NJ, p. 44 (1993).

176. Y. Matsuda, M. Morita and M. Ishikawa, Extended Abstracts, 183rd Meeting of The Electrochemical Society, Inc., May 16-21, 1993, Honolulu, HI, Abstract #63, p. 94.

177. O. Yamamoto, Y. Takeda, R. Kanno, and N. Imanishi, Extended Abstracts, 183rd Meeting of The Electrochemical Society, Inc., May 16-21, 1993, Honolulu, HI, Abstract #75, p. 112.

178. Y. Matsuda, M. Morita and M. Ishikawa, in Proceedings of the Symposium on New Sealed Rechargeable Batteries and Supercapacitors, B. Barnett, E. Dowgiallo, G. Halpert, Y. Matsuda, and Z. Takehara, eds., The Electrochemical Society Inc., Pennington, NJ, p. 206 (1993).

179. T. Uchida, Y. Morikawa, H. Ikuta and M. Wakihara, in Proceedings of the Symposium on New Sealed Rechargeable Batteries and Supercapacitors, B. Barnett, E. Dowgiallo, G. Halpert, Y. Matsuda, and Z. Takehara, eds., The Electrochemical Society Inc., Pennington, NJ, p. 292 (1993).

180. M. Morita, N. Nishimura and Y. Matsuda, Electrochim. Acta, **38**, 1721 (1993).

181. M. Ishikawa, M. Morita, M. Asao, Y. Matsuda, J. Electrochem. Soc., **141**, 1105 (1994).

182. M. Morita, M. Ishikawa and Y. Matsuda, in Proceedings of the Symposium on Materials for Electrochemical Energy Storage and Conversion-Batteries, Capacitors and Fuel Cells, Mater. Res. Soc. Symp. Proc. 393, D. Doughty, B. Vjas, T. Takamura and J. Huff, eds., MRS, Pittsburgh, PA, p. 195 (1995).

183. T. Takamura, M. Kikuchi, H. Awano, T. Ura and Y. Ikezawa, in Proceedings of the Symposium on Materials for Electrochemical Energy Storage and Conversion-Batteries, Capacitors and Fuel Cells, Mater. Res. Soc. Symp. Proc. 393, D. Doughty, B. Vjas, T. Takamura and J. Huff, eds., MRS, Pittsburgh, PA, p. 345 (1995).

184. T. Tamaki,in Proceedings of the Symposium on Materials for Electrochemical Energy Storage and Conversion-Batteries, Capacitors and Fuel Cells, Mater. Res. Soc. Symp. Proc. 393, D. Doughty, B. Vjas, T. Takamura and J. Huff, eds., MRS, Pittsburgh, PA, p. 357 (1995).

185. M. Verbrugge and B. Koch, J. Electrochem. Soc., **143**, 24 (1996).

186. L. Sawtschenko, K. Jobst, M. Schwarzenberg, L. Wuckel, and G. Paasch, Synth. Met., **41-43**, 1165 (1991).

187. K. Sekai, H. Azuma, A. Omaru, S. Fujita, H. Imoto, T. Endo, K. Yamaura, S. Mashiko, M. Yokogawa and Y. Nishi, presented at the 6th International Meeting on Lithium Batteries, Munster, Germany, May 10-15, 1992.

188. S. Yata, H. Kinoshita, M. Komori, N. Ando, N. T. Kashiwamura, T. Harada, T. K. Tanaka and T. Yamabe, Synth. Met., **62**, 153 (1994).

189. H. Imoto, A. Omaru, H. Azuma and Y. Nishi, in Proceedings of the Symposium on Lithium Batteries, S. Surampudi and V. Koch, eds., The Electrochemical Society Inc., Pennington, NJ, p. 9 (1993).

190. A. Omaru, H. Azuma, M. Aoki, A. Kita and Y. Nishi, in Proceedings of the Symposium on Lithium Batteries, S. Surampudi and V. Koch, eds., The Electrochemical Society Inc., Pennington, NJ, p. 21 (1993).

191. X. Chu, L. Schmidt and W. Smyrl, in Proceedings of the Symposium on Rechargeable Lithium and Lithium-Ion Batteries, S. Megahed, B. Barnett and L. Xie, eds., The Electrochemical Society Inc., Pennington, NJ, p. 196 (1994).

192. Y. Matsuda, M. Ishikawa, T. Nakamura and M. Morita, Extended Abstracts, 186th Meeting of The Electrochemical Society, Inc., October 9-14, 1994, Miami, FL., Abstract #86, p. 133.

193. K. Tokumitsu, A. Mabuchi, H. Fujimoto and T. Kasuh, J. Power Sources, **54**, 444 (1995); in Proceedings of the Symposium on Rechargeable Lithium and Lithium-Ion Batteries, S. Megahed, B. Barnett and L. Xie, eds., The Electrochemical Society Inc., Pennington, NJ, p. 136 (1994).

194. M. Alamgir, Q. Zuo and K. Abraham, J. Electrochem. Soc., **141**, L143 (1994).

195. T. Tran, J. Feikert, R. Pekala, J. Miller and B. Dunn, Mater. Res. Soc. Symp. Proc., **371** (Advances in Porous Materials), 449 (1995).

196. S. Yata, Y. Hato, H. Kinoshita, N. Ando, A. Anekawa, T. Hashimoto, M. Yamaguchi, K. Tanaka and T. Yamabe, Synth. Met., **73**, 273 (1995); S. Yata, T. Osaki, Y. Hato, T. Noguyoshi and H. Kinoshita, Synth. Met.., **38**, 177 (1990).

197. S. Yata, in Proceedings of the Symposium on Materials for Electrochemical Energy Storage and Conversion-Batteries, Capacitors and Fuel Cells, Mater. Res. Soc. Symp. Proc. 393, D. Doughty, B. Vjas, T. Takamura and J. Huff, eds., MRS, Pittsburgh, PA, p. 169 (1995).

198. J. Xue, K. Myrtle and J. Dahn, J. Electrochem. Soc., **142**, 2927 (1995).

199. M. Hara, A. Satoh, N. Takami and T. Ohsaki, J. Phys. Chem., **99**, 16338 (1995).

200. J. Xue and J. Dahn, J. Electrochem. Soc., **142**, 3668 (1995).

201. K. Hashizume, M. Tsutsui, T. Kaneko, S. Otani and S. Yoshimura, in Proceedings of the Symposium on Materials for Electrochemical Energy Storage and Conversion-Batteries, Capacitors and Fuel Cells, Mater. Res. Soc. Symp. Proc. 393, D. Doughty, B. Vjas, T. Takamura and J. Huff, eds., MRS, Pittsburgh, PA, p. 333 (1995).

202. M. Endo, Y. Nishimura, T. Takahashi, K. Takeuchi and M. Dresselhaus, J. Phys. Chem. Solids, **57**, 725 (1996).

203. W. Xing, J. Xue, T. Zheng, A. Gibaud and J. Dahn, J. Electrochem. Soc., **143**, 3482 (1996).

204. A. Satoh, N. Takami and T. Ohsaki, Solid State Ionics, **80**, 291 (1995).

205. K. Tatsumi, A. Mabuchi, N. Iwashita, H. Sakaebe, H. Shioyama, H. Fujimoto, and S. Higuchi, in Proceedings of the Symposium on Batteries and Fuel Cells for Stationary

and Electric Vehicle Applications, A. Landgrebe and Z. Takehara, eds., The Electrochemical Society Inc., Pennington, NJ, p. 64 (1993).

206. H. Fujimoto, A. Mabuchi, K. Tokumitsu and T. Kasuh, J. Power Sources, **54**, 440 (1995).

207. Y. Yoshimoto, H. Wada, H. Nakaya, M. Yoshida and S. Nakajima, Synth. Met., **41-43**, 2707 (1991).

208. B. Way and J. Dahn, J. Electrochem. Soc., **141**, 907 (1994).

209. M. Ishikawa, M. Morita, T. Hanada, Y. Matsuda and M. Kawaguchi, Denki Kagaku, **61**, 1395 (1993).

210. W. Weydanz, B. Way, T. Vanbuuren and J. Dahn, J. Electrochem. Soc., **141**, 900 (1994).

211. A. Wilson and J. Dahn, J. Electrochem. Soc., **142**, 326 (1995).

212. A. Wilson and J. Dahn, in Proceedings of the Symposium on Rechargeable Lithium and Lithium-Ion Batteries, S. Megahed, B. Barnett and L. Xie, eds., The Electrochemical Society Inc., Pennington, NJ, p. 158 (1994).

213. M. Ishikawa, T. Nakamura, M. Morita, Y. Matsuda and M. Kawaguchi, Denki Kagaku, **62**, 897 (1994).

214. F. Coowar, D. Billaud, J. Ghanbaja and P. Baudry, J. Power Sources, **62**, 179 (1996).

215. H. Nakamura, H. Komatsu and M. Yoshio J. Power Sources, **62**, 219 1(996).

216. Y. EinEli, S. Thomas, V. Koch, D. Aurbach, B. Markovsky and A. Schechter, J. Electrochem. Soc., **143**, L273 (1996).

217. M. Wakihara, Functional Materials, **14**, 5 (1994).

218. T. D. Tran, W. M. Goldberger, X. Song and K. Kinoshita, in Proceedings of the 8th International Meeting on Lithium Batteries, June 16-21, 1996, Nagoya, Japan (1996) p. 105; to be published in J. Power Sources, (1997).

219. J. Maire and J. Mering, in Industrial Carbon and Graphite, Society of Chemical Industry, London, p. 204 (1958); in Proceedings of the Fourth Conference on Carbon, Pergamon Press, New York, p. 345 (1960).

220. A. Dey, J. Electrochem. Soc., **118**, 1547 (1971).

221. D. Fauteux and R. Koksbang, J. Appl. Electrochem., **23**, 1 (1993).

222. D. Rahner, S. Machill, H. Schlorb, K. Siury, M. Kloss and W. Plieth, Solid State Ionics, **86-88**, 891 (1996)

223. J. Yang, M. Winter and J. Besenhard, Solid State Ionics, **90**, 281 (1996).

224. ITE Battery Newsletter, No. 4, p. 5 (July-Aug. 1996); information available (January 1997) on World-Wide Web site: http://www.fujifilm.co.jp/eng/news_e/nr079.html.

225. I. Courtney and J. Dahn, J. Electrochem. Soc., **144**, 2045 (1997).

226. Y. Idota, T. Kubota, A. Matsufuji, Y. Maekawa and T. Miyasaka, Science, **276**, 1395 (1997).

227. J. Isidorsson, C. Granqvist, L. Haggstrom and E. Nordstrom, J. Appl. Phys., **80**, 2367 (1996).

228. J. Isidorsson, M. Stromme, R. Gahlin, G. Miklasson and C. Granqvist, Solid State Commun., **99**, 109 (1996).

229. M. Stromme, J. Isidorsson, G. Miklasson and C. Granqvist, J. Appl. Phys., **80**, 233 (1996).

230. P. Olivi, E. Pereira, E. Longo, J. Varella and L. Bulhoes, J. Electrochem. Soc., **140**, L81 (1993).

231. B. Orel, U. Lavrencic-Stangar and K. Kalcher, J. Electrochem. Soc., **41**, L127 (1994).

232. J. Sarradin, A. Guessous and M. Ribes, J. Power Sources, **62**, 149 1(996).

233. C. Sigala, D. Guyomard, Y. Piffard and M. Tournoux, C.R. Acad. Sci. Serie II., **320**, 523 (1995).

234. J. Chen, Y. Li, W. Hurng and S. Whittingham, "Secondary Lithium Battery Using a New Layered Anode Material," Industrial Technology Research Institute, Taiwan, U. S. Patent 5,514,490 (May 7, 1996).

235. E. Ferg, R. Gummow, A de Kock and M. Thackeray, J. Electrochem. Soc., **41**, L147 (1994).

236. M. Nishijima, T. Kagohashi, M. Imanishi, Y. Takeda, O. Yamamoto and S. Kondo, Solid State Ionics, **83**, 107 (1996).

237. R. Yazami and M. Munshi, in Handbook of Solid State Batteries and Capacitors, M. Munshi, ed., World Scientific, Singapore, p. 425 (1995).

Ernest Orlando Lawrence Berkeley National Laboratory
One Cyclotron Road | Berkeley, California 94720

Prepared for the U.S. Department of Energy under Contract No. DE-AC03-76SF00098